DISCUSSION

In this study, we categorized high-grade gliomas into two groups, high-grade astrocytomas and high-grade oligodendroglial tumors, based on the presence of OC. Previous studies demonstrated that the survival of patients with AOA or AO is significantly longer than that of patients with AA (21,25,26,28,41), and some studies found that GBM with OC tends to have a better prognosis than ordinary GBM (12,34–37). In our series, 14 of 87 GBMs contained OC (16%). This result is similar to previous reports (34,35). Kraus et al. (36) mentioned that the physician ordering the patient's adjuvant treatment becomes altered to the better prognosis because of the high likelihood for a favorable response to chemotherapy in the presence of OC in a GBM. He et al. (34) found that the molecular profile associated with GBM with OC was different from that of ordinary GBM with frequent loss of heterozygosity on 1p and 19q. They suggested that GBM with OC represents a subgroup of tumors of oligodendroglial origin that is distinct from ordinary GBM in terms of the tumorigenesis pathway (34). By subanalysis of a clinical randomized trial of RTOG 83-02, Donahue et al. (25) suggested that high-grade gliomas with OC should be considered in the design and stratification of malignant glioma trials, because patients who have high-grade gliomas with OC have the potential for prolonged survival.

The primary aim of this retrospective analysis was to evaluate the impact of the extent of tumor resection in high-grade astrocytomas and high-grade oligodendroglial tumors. Previous studies demonstrated that complete resection of pre-operative contrast enhancing lesions improves survival in

Table 4. Univariate analysis of clinical and tumor parameters with OS and PFS in 67 patients with high-grade oligodendroglial tumors

	Overall survival			Progression-free survival		
	Hazard ratio	95% CI	*P* value	Hazard ratio	95% CI	*P* value
Age[a]	1.072	1.03–1.12	0.001	1.039	1.01–1.07	0.005
Pre-operative KPS						
<80	2.373	0.89–6.35	0.09	1.829	0.84–3.97	0.13
≥80	1.0			1.0		
Tumor diameter						
>4 cm	2.640	0.88–7.97	0.08	1.985	0.95–4.12	0.07
≤4 cm	1.0			1.0		
Eloquent area						
No	0.781	0.31–1.99	0.60	0.669	0.34–1.33	0.25
Yes	1.0			1.0		
WHO grading						
Grade III	0.321	0.12–0.83	0.02	0.453	0.21–0.96	0.04
Grade IV	1.0			1.0		
Post-operative TMZ						
No	0.640	0.22–1.84	0.41	0.811	0.38–1.75	0.59
Yes	1.0			1.0		

[a]Increasing variable.

Table 5. Multivariate analysis of EOR affecting OS and PFS in 67 patients with high-grade oligodendroglial tumors[a]

	Overall survival			Progression-free survival		
	Hazard ratio	95% CI	*P* value	Hazard ratio	95% CI	*P* value
Complete resection	0.878	0.24–3.25	0.85	0.517	0.21–1.30	0.16
Incomplete resection	1.0			1.0		
Biopsy	9.35	2.52–34.8	<0.001	3.718	1.45–9.54	0.006

[a]Adjusting for the effect of patient age, pre-operative Karnofsky performance scale, tumor size (maximum diameter) and histological WHO grading.

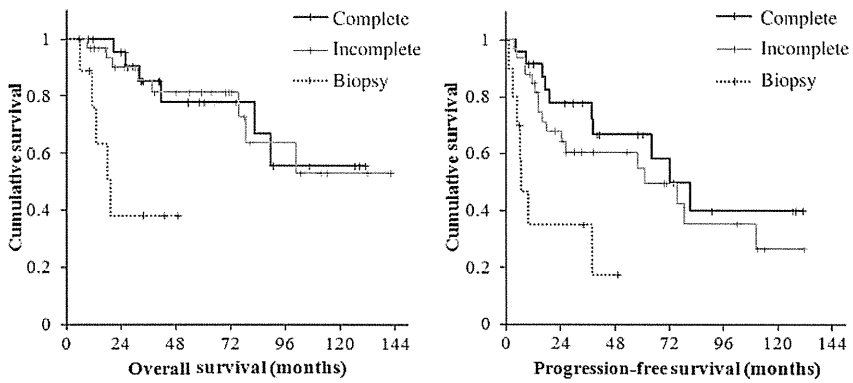

Figure 3. Overall (left) and progression-free (right) survival analysis for patients with high-grade oligodendroglial tumor demonstrated as the Kaplan–Meier plots by the extent of surgical resection (complete resection, incomplete resection and biopsy alone).

GBMs and AAs (1,7–9,11,13–16). With volumetric analysis on AAs, Keles et al. (16) reported that post-operative residual contrast enhancement has a statistically significant unfavorable effect on survival. McGirt et al. (11) reported that gross total resection of contrast enhancement was independently associated with increased survival over subtotal resection in AA. Lacroix et al. (9) found that greater than 98% tumor resection was significantly associated with improved survival in newly diagnosed GBMs. In the present study, radiographically complete resection of enhancing lesions with early post-operative MR imaging was an independently good prognostic factor of both OS and PFS in high-grade astrocytomas in accordance with previous studies. Patients with residual enhancement on post-operative MR imaging did not have a survival benefit compared with patients who underwent biopsy alone. Our data confirmed that extensive surgery plays an important role in predicting the risk of progression and death in high-grade astrocytomas.

In this series of the patients with high-grade astrocytoma, the prognosis is not significantly different between AAs (WHO Grade III tumors) and GBMs (WHO Grade IV tumors). This result is intriguing. In reassessment of histopathology according to the WHO 2007 criteria, our neuropathologists classified high-grade oligodendroglial tumors regardless of the definite numeric value for the oligodendroglial tumor component portion. Patients who have AA with OC have the potential for prolonged (25); therefore, it is conceivable that the prognostic outcome of our patients with pure AA was relatively poor compared with previous reports. We suppose that the further investigation to increase the number of cases for AA which was rather less than that of GBM might be required. In addition, age and pre-operative KPS were also unrelated to the prognosis in the patients with high-grade astrocytomas. In this series, eligible patients were only able to undergo post-operative radiotherapy, so pessimistic patients with poor prognosis who could not undergo radiotherapy, i.e. very elderly or very poor preoperative KPS score, were excluded. Thus, prognosis might be less affected by age and pre-operative KPS.

There are a relatively small number of studies evaluating the relationship between the EOR and prognosis on high-grade gliomas with OC (17,18,20,42). In our patients with high-grade oligodendroglial tumors, including GBMs with OC, complete resection versus incomplete resection was not associated with survival in multivariate analysis. There was a trend toward longer PFS with complete resection, although the difference between complete resection and incomplete resection did not reach statistical significance ($P = 0.16$). Patients who underwent tumor resection (including both complete and incomplete resection) had significantly improved OS and PFS compared with patients who underwent biopsy alone (OS: $P < 0.001$ and PFS: $P = 0.006$, biopsy versus incomplete resection in multivariate analysis). In the subanalysis of Phase III trials for AOs and AOAs, tumor-debulking surgery was independently associated with longer OS time (18,42). The degree of resection was not distinct in these trials; therefore, our result is expected to be similar. Oligodendroglial tumors are well known to be generally chemosensitive tumor (30–33), leading to be better prognosis regardless of the extent of tumor resection compared with astrocytic tumor. In fact, in the present series, an objective response was obtained 24 cases (63%) among 38 high-grade oligodendroglial tumor patients with post-operative residual tumor (incomplete resection or biopsy), while an objective response was obtained 12 cases (24%) among 51 patients with high-grade astrocytoma patients with post-operative residual tumor [response to chemotherapy is assessed on the basis of criteria proposed by Macdonald et al. (43), and objective response defined as complete response or partial response]. Although the role of extensive surgery remains uncertain in high-grade oligodendroglial tumors, maximum safe resection should contribute to prolong survival even if the lesion involves eloquent areas.

CONCLUSION

Our data suggest that maximal cytoreduction should be attempted in high-grade gliomas regardless of histological subtype or tumor location. However, the impact of the EOR in high-grade astrocytomas might be different from that in high-grade oligodendroglial tumors. Certainly, this study has some limitations. This study is inherently limited by its retrospective design and the limited number of patients. In addition, there were relatively few deaths in patients with high-grade oligodendroglial tumors, which limited extensive multivariate analysis. However, when novel examinations enable us to confirm histological diagnosis pre-operatively, we anticipate that our present data may be important for the surgical strategy of high-grade gliomas.

Conflict of interest statement

None declared.

References

1. Stummer W, Pichlmeier U, Meinel T, Wiestler OD, Zanella F, Reulen HJ. Fluorescence-guided surgery with 5-aminolevulinic acid for resection of malignant glioma: a randomised controlled multicentre phase III trial. *Lancet Oncol* 2006;7:392–401.
2. Stummer W, Reulen HJ, Meinel T, Pichlmeier U, Schumacher W, Tonn JC, et al. Extent of resection and survival in glioblastoma multiforme: identification of and adjustment for bias. *Neurosurgery* 2008;62:564–76.
3. Yoshikawa K, Kajiwara K, Morioka J, Fujii M, Tanaka N, Fujisawa H, et al. Improvement of functional outcome after radical surgery in glioblastoma patients: the efficacy of a navigation-guided fence-post procedure and neurophysiological monitoring. *J Neurooncol* 2006;78:91–7.
4. Kombos T, Picht T, Derdilopoulos A, Suess O. Impact of intraoperative neurophysiological monitoring on surgery of high-grade gliomas. *J Clin Neurophysiol* 2009;26:422–5.
5. Muragaki Y, Iseki H, Maruyama T, Kawamata T, Yamane F, Nakamura R, et al. Usefulness of intraoperative magnetic resonance imaging for glioma surgery. *Acta Neurochir Suppl* 2006;98:67–75.

6. Senft C, Franz K, Blasel S, Oszvald A, Rathert J, Seifert V, et al. Influence of iMRI-guidance on the extent of resection and survival of patients with glioblastoma multiforme. *Technol Cancer Res Treat* 2010;9:339–46.
7. Keles GE, Anderson B, Berger MS. The effect of extent of resection on time to tumor progression and survival in patients with glioblastoma multiforme of the cerebral hemisphere. *Surg Neurol* 1999;52:371–9.
8. Kowalczuk A, Macdonald RL, Amidei C, Dohrmann G, 3rd, Erickson RK, Hekmatpanah J, et al. Quantitative imaging study of extent of surgical resection and prognosis of malignant astrocytomas. *Neurosurgery* 1997;41:1028–36.
9. Lacroix M, Abi-Said D, Fourney DR, Gokaslan ZL, Shi W, DeMonte F, et al. A multivariate analysis of 416 patients with glioblastoma multiforme: prognosis, extent of resection, and survival. *J Neurosurg* 2001;95:190–8.
10. Lamborn KR, Chang SM, Prados MD. Prognostic factors for survival of patients with glioblastoma: recursive partitioning analysis. *Neuro Oncol* 2004;6:227–35.
11. McGirt MJ, Chaichana KL, Gathinji M, Attenello FJ, Than K, Olivi A, et al. Independent association of extent of resection with survival in patients with malignant brain astrocytoma. *J Neurosurg* 2009;110:156–62.
12. Pope WB, Sayre J, Perlina A, Villablanca JP, Mischel PS, Cloughesy TF. MR imaging correlates of survival in patients with high-grade gliomas. *Am J Neuroradiol* 2005;26:2466–74.
13. Ushio Y, Kochi M, Hamada J, Kai Y, Nakamura H. Effect of surgical removal on survival and quality of life in patients with supratentorial glioblastoma. *Neurol Med Chir (Tokyo)* 2005;45:454–60.
14. Nitta T, Sato K. Prognostic implications of the extent of surgical resection in patients with intracranial malignant gliomas. *Cancer* 1995;75:2727–31.
15. Stark AM, Nabavi A, Mehdorn HM, Blomer U. Glioblastoma multiforme-report of 267 cases treated at a single institution. *Surg Neurol* 2005;63:162–9.
16. Keles GE, Chang EF, Lamborn KR, Tihan T, Chang CJ, Chang SM, et al. Volumetric extent of resection and residual contrast enhancement on initial surgery as predictors of outcome in adult patients with hemispheric anaplastic astrocytoma. *J Neurosurg* 2006;105:34–40.
17. Puduvalli VK, Hashmi M, McAllister LD, Levin VA, Hess KR, Prados M, et al. Anaplastic oligodendrogliomas: prognostic factors for tumor recurrence and survival. *Oncology* 2003;65:259–66.
18. van den Bent MJ, Carpentier AF, Brandes AA, Sanson M, Taphoorn MJ, Bernsen HJ, et al. Adjuvant procarbazine, lomustine, and vincristine improves progression-free survival but not overall survival in newly diagnosed anaplastic oligodendrogliomas and oligoastrocytomas: a randomized European Organisation for Research and Treatment of Cancer phase III trial. *J Clin Oncol* 2006;24:2715–22.
19. Kristof RA, Neuloh G, Hans V, Deckert M, Urbach H, Schlegel U, et al. Combined surgery, radiation, and PCV chemotherapy for astrocytomas compared to oligodendrogliomas and oligoastrocytomas WHO grade III. *J Neurooncol* 2002;59:231–7.
20. Jeremic B, Milicic B, Grujicic D, Samardzic M, Antunovic V, Dagovic A, et al. Combined treatment modality for anaplastic oligodendroglioma and oligoastrocytoma: a 10-year update of a phase II study. *Int J Radiat Oncol Biol Phys* 2004;59:509–14.
21. Tortosa A, Vinolas N, Villa S, Verger E, Gil JM, Brell M, et al. Prognostic implication of clinical, radiologic, and pathologic features in patients with anaplastic gliomas. *Cancer* 2003;97:1063–71.
22. Bauman G, Fisher B, Watling C, Cairncross JG, Macdonald D. Adult supratentorial low-grade glioma: long-term experience at a single institution. *Int J Radiat Oncol Biol Phys* 2009;75:1401–7.
23. Pignatti F, van den Bent M, Curran D, Debruyne C, Sylvester R, Therasse P, et al. Prognostic factors for survival in adult patients with cerebral low-grade glioma. *J Clin Oncol* 2002;20:2076–84.
24. Shaw E, Arusell R, Scheithauer B, O'Fallon J, O'Neill B, Dinapoli R, et al. Prospective randomized trial of low- versus high-dose radiation therapy in adults with supratentorial low-grade glioma: initial report of a North Central Cancer Treatment Group/Radiation Therapy Oncology Group/Eastern Cooperative Oncology Group study. *J Clin Oncol* 2002;20:2267–76.
25. Donahue B, Scott CB, Nelson JS, Rotman M, Murray KJ, Nelson DF, et al. Influence of an oligodendroglial component on the survival of patients with anaplastic astrocytomas: a report of Radiation Therapy Oncology Group 83–02. *Int J Radiat Oncol Biol Phys* 1997;38:911–4.
26. Ino Y, Zlatescu MC, Sasaki H, Macdonald DR, Stemmer-Rachamimov AO, Jhung S, et al. Long survival and therapeutic responses in patients with histologically disparate high-grade gliomas demonstrating chromosome 1p loss. *J Neurosurg* 2000;92:983–90.
27. Shaw EG, Scheithauer BW, O'Fallon JR, Davis DH. Mixed oligoastrocytomas: a survival and prognostic factor analysis. *Neurosurgery* 1994;34:577–82.
28. Park CK, Lee SH, Han JH, Kim CY, Kim DW, Paek SH, et al. Recursive partitioning analysis of prognostic factors in WHO grade III glioma patients treated with radiotherapy or radiotherapy plus chemotherapy. *BMC Cancer* 2009;9:450.
29. Shaw EG, Scheithauer BW, O'Fallon JR. Supratentorial gliomas: a comparative study by grade and histologic type. *J Neurooncol* 1997;31:273–8.
30. Cairncross G, Macdonald D, Ludwin S, Lee D, Cascino T, Buckner J, et al. Chemotherapy for anaplastic oligodendroglioma. National Cancer Institute of Canada Clinical Trials Group. *J Clin Oncol* 1994;12:2013–21.
31. Cairncross JG, Macdonald DR. Successful chemotherapy for recurrent malignant oligodendroglioma. *Ann Neurol* 1988;23:360–4.
32. Cairncross JG, Ueki K, Zlatescu MC, Lisle DK, Finkelstein DM, Hammond RR, et al. Specific genetic predictors of chemotherapeutic response and survival in patients with anaplastic oligodendrogliomas. *J Natl Cancer Inst* 1998;90:1473–9.
33. Smith JS, Perry A, Borell TJ, Lee HK, O'Fallon J, Hosek SM, et al. Alterations of chromosome arms 1p and 19q as predictors of survival in oligodendrogliomas, astrocytomas, and mixed oligoastrocytomas. *J Clin Oncol* 2000;18:636–45.
34. He J, Mokhtari K, Sanson M, Marie Y, Kujas M, Huguet S, et al. Glioblastomas with an oligodendroglial component: a pathological and molecular study. *J Neuropathol Exp Neurol* 2001;60:863–71.
35. Homma T, Fukushima T, Vaccarella S, Yonekawa Y, Di Patre PL, Franceschi S, et al. Correlation among pathology, genotype, and patient outcomes in glioblastoma. *J Neuropathol Exp Neurol* 2006;65:846–54.
36. Kraus JA, Lamszus K, Glesmann N, Beck M, Wolter M, Sabel M, et al. Molecular genetic alterations in glioblastomas with oligodendroglial component. *Acta Neuropathol* 2001;101:311–20.
37. Hilton DA, Penney M, Pobereskin L, Sanders H, Love S. Histological indicators of prognosis in glioblastomas: retinoblastoma protein expression and oligodendroglial differentiation indicate improved survival. *Histopathology* 2004;44:555–60.
38. Bauman GS, Ino Y, Ueki K, Zlatescu MC, Fisher BJ, Macdonald DR, et al. Allelic loss of chromosome 1p and radiotherapy plus chemotherapy in patients with oligodendrogliomas. *Int J Radiat Oncol Biol Phys* 2000;48:825–30.
39. Chang EF, Smith JS, Chang SM, Lamborn KR, Prados MD, Butowski N, et al. Preoperative prognostic classification system for hemispheric low-grade gliomas in adults. *J Neurosurg* 2008;109:817–24.
40. Stupp R, Mason WP, van den Bent MJ, Weller M, Fisher B, Taphoorn MJ, et al. Radiotherapy plus concomitant and adjuvant temozolomide for glioblastoma. *N Engl J Med* 2005;352:987–96.
41. Miller CR, Dunham CP, Scheithauer BW, Perry A. Significance of necrosis in grading of oligodendroglial neoplasms: a clinicopathologic and genetic study of newly diagnosed high-grade gliomas. *J Clin Oncol* 2006;24:5419–26.
42. Cairncross G, Berkey B, Shaw E, Jenkins R, Scheithauer B, Brachman D, et al. Phase III trial of chemotherapy plus radiotherapy compared with radiotherapy alone for pure and mixed anaplastic oligodendroglioma: Intergroup Radiation Therapy Oncology Group Trial 9402. *J Clin Oncol* 2006;24:2707–14.
43. Macdonald DR, Cascino TL, Schold SC, Jr, Cairncross JG. Response criteria for phase II studies of supratentorial malignant glioma. *J Clin Oncol* 1990;8:1277–80.

OPEN ACCESS Freely available online

PLoS one

Prognostic Implication of Histological Oligodendroglial Tumor Component: Clinicopathological Analysis of 111 Cases of Malignant Gliomas

Hiromi Kanno[1], Hiroshi Nishihara[2]*, Takuhito Narita[1], Shigeru Yamaguchi[3], Hiroyuki Kobayashi[3], Mishie Tanino[1], Taichi Kimura[1], Shunsuke Terasaka[3], Shinya Tanaka[1]

1 Laboratory of Cancer Research, Department of Pathology, Hokkaido University School of Medicine, Sapporo, Japan, **2** Laboratory of Translational Pathology, Hokkaido University School of Medicine, Sapporo, Japan, **3** Department of Neurosurgery, Hokkaido University School of Medicine, Sapporo, Japan

Abstract

The favorable prognosis of high-grade oligodendroglial tumor such as glioblastoma (GBM) with oligodendroglioma component (GBMO) has been suggested; however, the studies which examine the prognostic significance of oligodendroglial tumor were limited. In this study, we performed a histopathology-based reevaluation of 111 cases of high grade gliomas according to the latest World Health Organization (WHO), and compared the clinical outcomes between oligodendroglial tumors and pure astrocytic tumors. The survival analysis revealed that the patients with high grade oligodendroglial tumor including GBMO significantly indicated better prognosis compared to the patients with high grade pure astrocytic tumors (GBM and AA, anaplastic astrocytoma) as expected, and the obtained survival curves were almost identical to those from the patients with conventional Grade III or Grade IV tumors, respectively. Moreover, if the cases of oligodendroglial tumor were histopathologically excluded, the patients with AA exhibited extremely poor prognosis which was similar to that of GBM, suggesting that the histological identification of oligodendroglial tumor component, even partially, prescribe the prognosis of high grade glioma patients. This is the prominent report of retrospective clinicopathological analysis for high-grade gliomas throughout Grade III and IV, especially referring to the prognostic value of histological oligodendroglial tumor component; in addition, our results might offer an alternative aspect for the grading of high-grade astrocytic/oligodendroglial tumors.

Citation: Kanno H, Nishihara H, Narita T, Yamaguchi S, Kobayashi H, et al. (2012) Prognostic Implication of Histological Oligodendroglial Tumor Component: Clinicopathological Analysis of 111 Cases of Malignant Gliomas. PLoS ONE 7(7): e41669. doi:10.1371/journal.pone.0041669

Editor: Mitsunobu R. Kano, University of Tokyo, Japan

Received February 24, 2012; **Accepted** June 24, 2012; **Published** July 24, 2012

Funding: The authors have no support or funding to report.

Competing Interests: The authors have declared that no competing interests exist.

* E-mail: hnishihara@s5.dion.ne.jp

Introduction

High grade gliomas/malignant gliomas are composed of astrocytic and/or oligodendroglial tumors which are categorized into WHO grade III and IV. The clinical outcome of the patients with these diseases remains extremely poor, although the oligodendroglial tumors are reported to exhibit relatively favorable prognosis compared to the astrocytic tumors [1,2,3]. In addition to variable prognostic factors such as the age of the patients, the extent of resection or postoperative radiation therapy, tumor grade and Karnofsky performance status (KPS) score, the presence of the oligodendroglial tumor component, prominent microvascular proliferation and/or necrosis in high-grade glioma are focused upon in the recent edition of WHO Classification (4th, 2007) [4]. "Glioblastoma with oligodendroglioma component" was placed into Grade IV, and anaplastic oligoastrocytoma (AOA) with microscopical necrosis, formerly categorized in Grade III, is also regarded as Grade IV. In recent reports, the survival analysis of Glioblastoma (GBM) vs. Glioblastoma with oligodendroglioma component (GBMO) was performed and showed no significance between them [5,6], although some other reports have indicated a better prognosis for GBMO [7,8,9,10]. In addition, a detailed survival analysis limited in Grade III gliomas, between oligodendroglial tumor (AO, AOA) and pure astrocytic tumor (Anaplastic astrocytoma, AA), has not been reported, especially after the recent edition of WHO Classification; therefore, the clinicopathological significance of the oligodendroglial tumor component is still controversial.

Here we reviewed and analyzed 111 cases of high grade gliomas based on the latest WHO classification, and found the critical implication between the prognosis and histological evaluation, especially the presence of the oligodendroglial tumor component.

Materials and Methods

Patients

This study was performed with the approval of the Internal Review Board on ethical issues of Hokkaido University Hospital and Graduate School of Medicine, Sapporo, Japan. The samples and the patients' information were obtained under a blanket written informed consent. Among the patients who were treated at the department of neurosurgery of Hokkaido University Hospital or its affiliated hospitals between 2000 and 2009, we had 133 cases of malignant gliomas (AA, AO, AOA, GBM and GBMO). We performed immunohistochemistry with anti-Olig2 and Glial fibrillary acidic protein (GFAP) antibodies during the initial

Table 1. Characteristics of 111 Patients.

Characteristics	Number of patients (%)
Median age (range)	57 (11–83)
Gender	
Male	64 (57.7)
Female	47 (42.3)
Extent of surgery	
Biopsy	22 (19.9)
Partial resection	26 (23.4)
Subtotal resection	21 (18.9)
Gross total resection	40 (36.0)
No data	2 (1.8)
Chemotherapy	
ACNU	50 (45.0)
TMZ	40 (36.0)
CDDP	2 (1.8)
CBDCA	1 (0.9)
None	17 (15.3)
No data	1 (0.9)
Radiation therapy	
Yes	101 (91.0)
No	9 (8.1)
No data	1 (0.9)
Preoperative KPS score	
80≥	72 (64.9)
80<	35 (31.5)
No data	4 (3.6)

ACNU: Nimustine hydrochloride, TMZ: Temozolomide, CDDP: Cisplatin, CBDCA: Carboplatin, KPS: Karnofsky performance status.
doi:10.1371/journal.pone.0041669.t001

diagnosis process for confirmation of glial tumor, and we observed all of the 111 case were positive for at least one of these two antibodies. The clinical outcomes of these patients were collected retrospectively. Among these patients, 22 cases were excluded because of following reasons; 13 patients had clinical or histopathological evidence of preceding low grade glioma, 7 patients' pathological diagnosis couldn't reach the final consensus and 2 patients' survival time wasn't available. The seven patients whose diagnoses couldn't be determined includes 4 cases with insufficient tissue volume, 1 case suspected as oligoastrocytoma, WHO Grade I, and 2 cases suspected as Primitive neuroectodermal tumor (PNET). There was no case which needs to be differentiated from metastatic carcinoma or other intracranial tumor. Finally, 111 cases were applied for the overall survival analysis. Among these 111 cases, the data of progression-free survival was available in 78 patients.

Histopathological Studies

Here we performed this analysis as a retrospective study. Pathological review of all surgical or biopsy specimens were performed by four pathologists (S.T, H.N, M.T and H.K) who were blind to the clinical information. Routinely formalin-fixed, Paraffin-embedded tissue sections of tumor were stained with Hematoxylin and eosin (H&E) and used for pathological review. Histological features including cellularity, cellular atypia, mitotic activity, necrosis, and microvascular proliferation were reevaluated and diagnosis was made according to the 2007 WHO classification. The oligodendroglial tumor component, such as the oligodendroglioma component in GBM, was defined as the presence of at least 5 tumor cells with obvious perinuclear halo in cluster or even in diffuse, scattered pattern in high power field of H&E section, and we did not refer to any immunohistochemical staining such as Olig-2 or GFAP. The cells which had round nuclei or a microcystic pattern without a perinuclear halo were not regarded as an oligodendroglial tumor component.

Table 2. Summary of the cases of altered diagnosis.

Initial diagnosis	Altered diagnosis	Number of patients
AA (14)	AO	1
	AOA	2
AO (9)	AOA	3
AOA (20)	AO	4
	GBMO	4
GBM (68)	AOA	1
	AA	2
	GBMO	13
Total (111)		30

AA: anaplastic astrocytoma, AO: anaplastic oligodendroglioma, AOA: anaplastic oligoastrocytoma, GBM: glioblastoma, GBMO: glioblastoma with oligodendroglioma component.
doi:10.1371/journal.pone.0041669.t002

FISH (Fluorescence in situ Hybridization) Analysis

Among the patients who underwent surgery between 2006 and 2009, eighteen samples were available for FISH analysis to detect the chromosome 1 (1p) deletion. The analysis was conducted using paraffin embedded tissue as previously described [11]. The fluorochrome-labeled probes mapping to 1p36 was used for the detection of 1p loss. Approximately 100 nonoverlapping nuclei were enumerated per hybridization. The deletion for 1p was defined as more than 30% of tumor nuclei containing 1 signal for 1p36.

Statistical Analysis

Time to progression and survival, measured from the date of first surgical resection or biopsy to disease progression and death, respectively, or the date of last follow-up visit was analyzed by the

Table 3. Final diagnosis of the 111 cases.

Histological subtype	Number of patients (%)
AO	11 (10)
AOA	18 (16)
GBMO	17 (15)
AA	13 (12)
GBM	52 (47)
Total	**111**

AA: anaplastic astrocytoma, AO: anaplastic oligodendroglioma, AOA: anaplastic oligoastrocytoma, GBM: glioblastoma, GBMO: glioblastoma with oligodendroglioma component.
doi:10.1371/journal.pone.0041669.t003

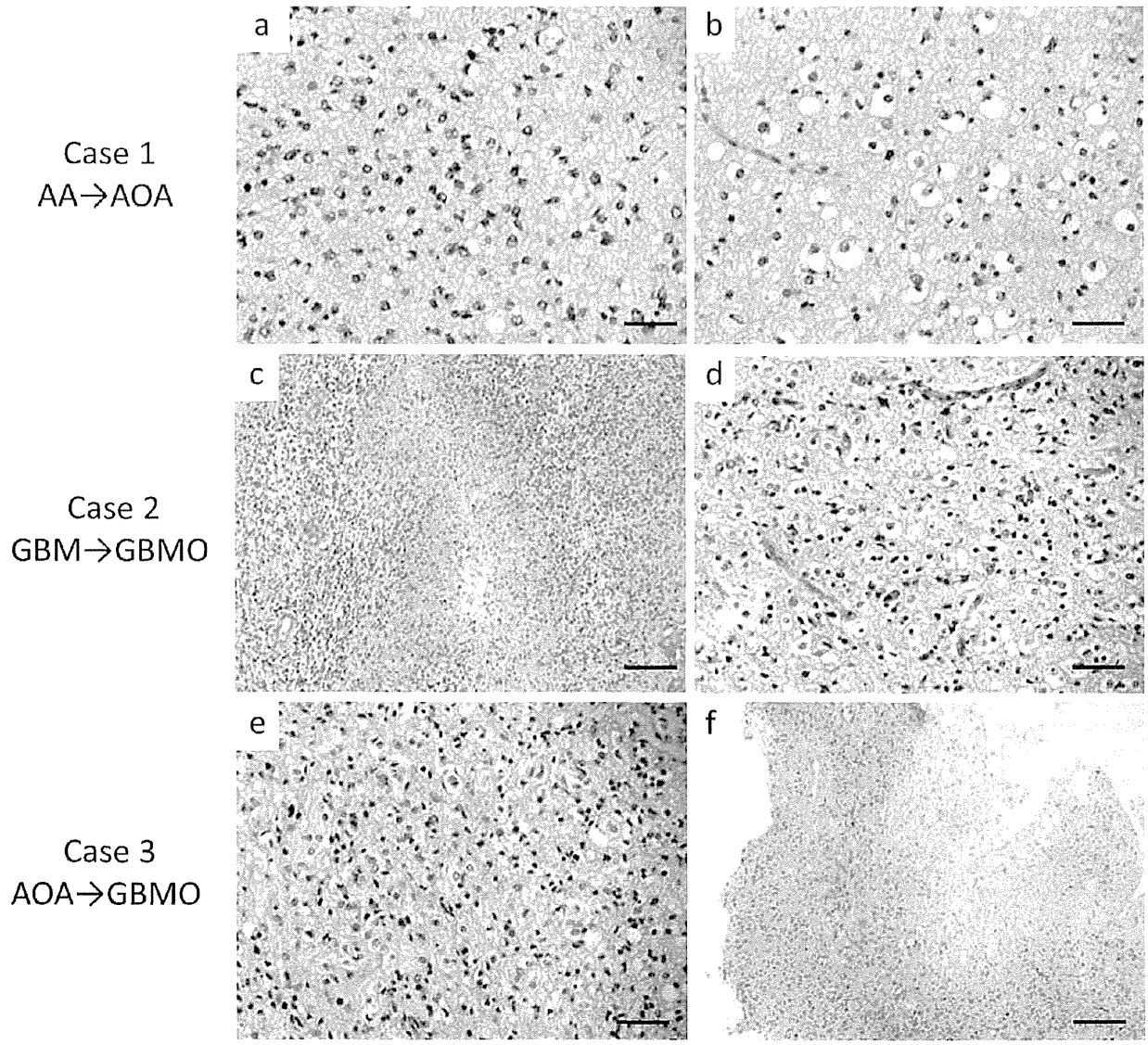

Figure 1. The histological appearance of the cases in which the diagnosis was altered. Case 1: The initial diagnosis was AA because of the prominent atypical astrocytic cells (a). After the histological review, an obvious oligodendroglial tumor component with perinuclear halo was identified (b), and the histological diagnosis was altered to AOA. Case 2: Dense infiltrate of atypical large tumor cells with necrosis indicate GBM (c). However, we found the oligodendroglioma component within the section (d), thereby changing the final diagnosis to GBMO according to the 2007 WHO classification. Case 3: The tumor consists of middle-sized atypical astrocytic cells with eosinophilic cytoplasm and also atypical oligodendroglial cells with perinuclear halo, giving the initial diagnosis as AOA (e). The cellularity and nuclear atypia of this case is moderate; however, the presence of micronecrosis (f) in this lesion enforced us to alter the diagnosis to GBMO. (The scale bars represent 50 μm (a, b, d, and e) and 100 μm (c, f).).
doi:10.1371/journal.pone.0041669.g001

Kaplan-Meier method. Log-rank test was employed for comparing the curves.

Results

Characteristics of Patients

The summary of included patients is shown in Table 1. Median age of the patients was 57 years (ranging from 11 to 83). Sixty-four patients were men and 47 were women. The treatments included surgical resection, adjuvant radiation and adjuvant chemotherapy. Twenty-two patients (19.9%) underwent biopsy, 26 patients (23.4%) underwent partial resection, 21 patients (18.9%) underwent subtotal resection and 40 patients (36.0%) underwent gross total resection, while the details of 2 patients (1.8%) were unknown. Among the 111 patients, 101 patients (91.0%) received radiation therapy: basically the patients with Grade III glioma received 54 Gy/27 fr, and patients with Grade IV glioma received 60 Gy/30 fr. Chemotherapy was applied to 50 patients (45.0%) with nimustine hydrochloride (ACNU), and 40 patients (36.0%) with temozolomide (TMZ), 2 patients (1.8%) with cisplatin (CDDP), and 1 patient (0.9%) with carboplatin (CBDCA), while 17 patients (15.3%) didn't receive any chemotherapy. The preoperative KPS score of 72 patients (64.9%) was more than

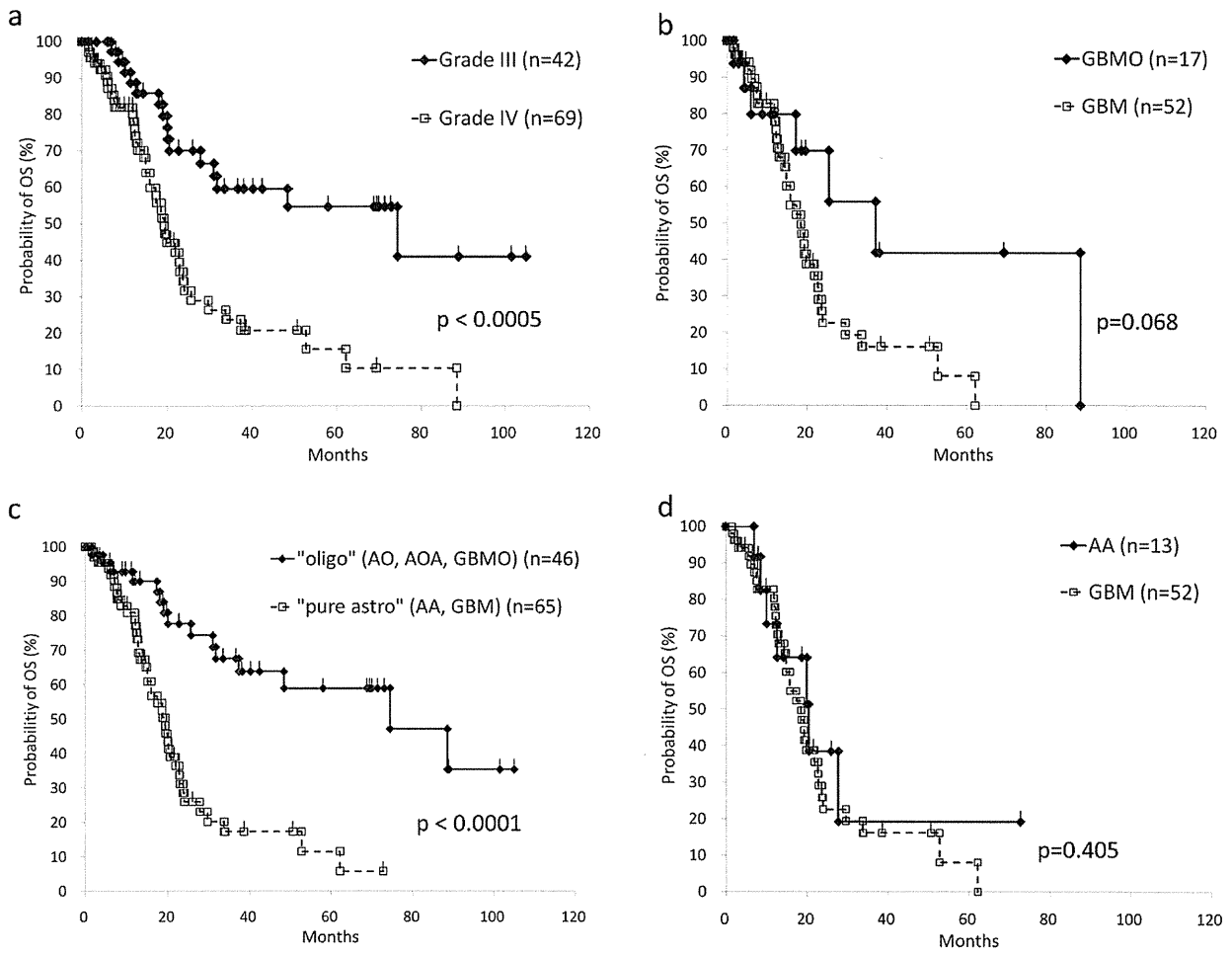

Figure 2. Overall survival (OS) analysis based on the histological subclassifications. a: Conventional Grade III gliomas (AA, AO and AOA) show significantly better prognosis than Grade IV gliomas (GBM, GBMO). b: GBMO presented longer survival compared to GBM, although it is statistically not significant (p = 0.068). c: Oligodendroglial tumor ("oligo"; AO, AOA, GBMO) shows significantly better prognosis compared to pure astrocytic tumor ("pure astro"; AA, GBM). d: The survival curve of AA patients is almost identical to that of GBM patients.
doi:10.1371/journal.pone.0041669.g002

80 and that of 35 patients (31.5%) was lower than 80. After the treatments, the patients were followed in the outpatient clinic until either their death or their last visit. The mean duration of the follow-up was 24.3 months (range, 0.7–105.0). The detailed information of 13 cases of AAs was as follows. Median age of the patients was 48.2 years (ranging from 15 to 68). Seven patients were men and 6 were women. Seven patients (53.8%) underwent biopsy, 3 patients (23.1%) underwent partial resection, 1 patient (7.7%) underwent subtotal resection and 2 patients (15.4%) underwent gross total resection. Among the 13 patients, 12 patients (92.3%) received radiation therapy. Chemotherapy was applied to all patients; 9 (69.2%) with nimustine hydrochloride (ACNU), and 4 patients (30.8%) with temozolomide (TMZ). The mean duration of the follow-up was 19.5 months (range, 6.9–72.7).

Histological Evaluation

Because the 111 studied cases of grade III and IV malignant gliomas included the cases diagnosed before 2007, we first performed a histological review of all 111 cases based on the recent edition of WHO Classification (4th, 2007) [4] to obtain the unified pathological diagnosis. As summarized in Table 2, the initial diagnosis of 30 cases of malignant glioma was altered: 17 cases of newly established GBMO were included, and 3 cases of AA were re-categorized into AO or AOA because of the presence of an obvious oligodendroglial lesion, resulting in the additional 17 cases of oligodendroglial tumors (AO, AOA and GBMO). We identified micronecrosis in the 4 cases of AOA; thus their diagnosis was altered to GBMO. The final pathological diagnosis after the review is summarized in Table 3. The histological appearance of the cases in which the pathological diagnosis was altered is exhibited in Fig. 1, while the typical histological appearances of high-grade gliomas (AA, AO, AOA and GBM) are shown in Fig. S1.

Survival Analysis Based on the Reviewed Pathological Diagnosis

The overall survival (OS) based on the conventional grading entities of gliomas, i.e. Grade III (AO, AOA and AA) versus Grade IV (GBM and GBMO) by the Kaplan-Meier method is shown in Fig. 2a, and is approximately similar to that described in previous

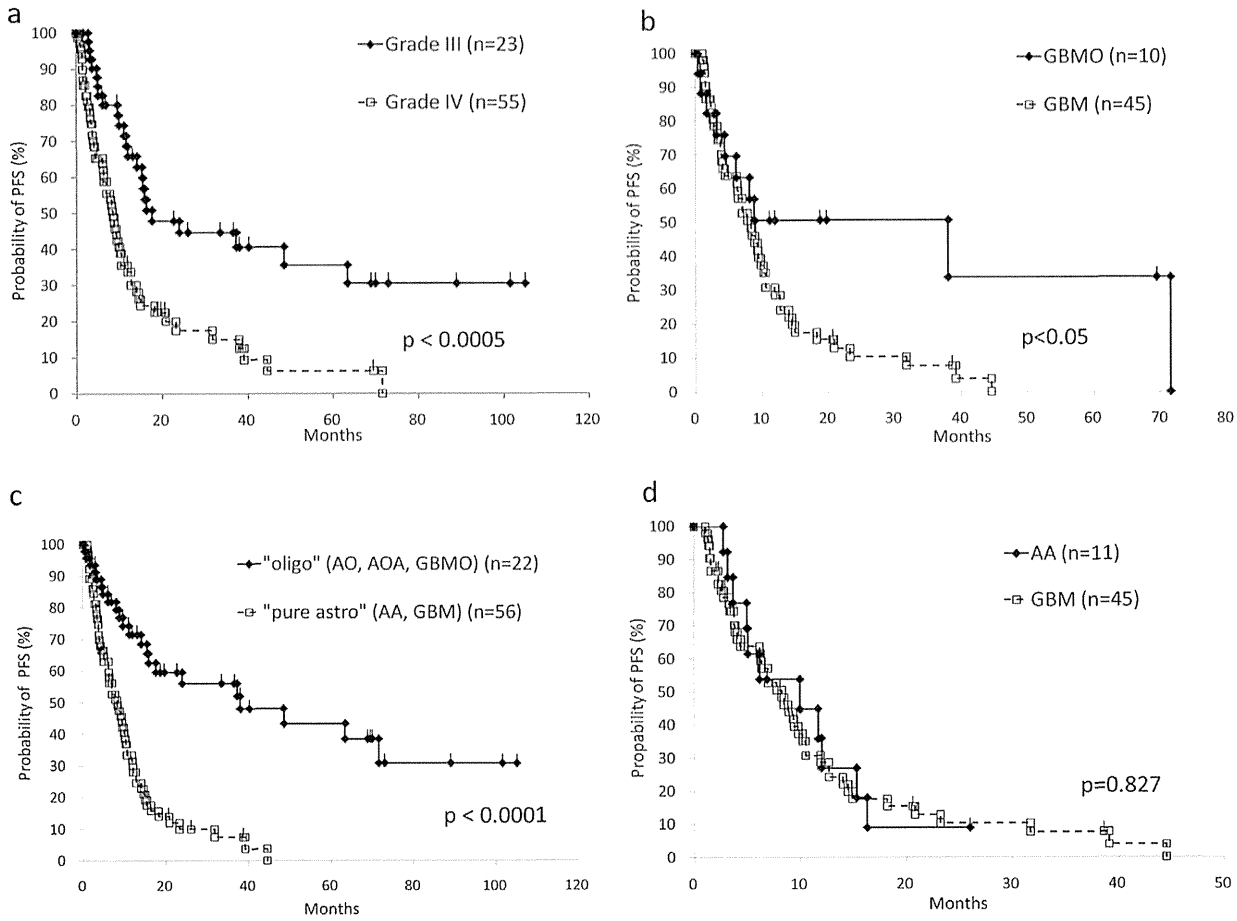

Figure 3. Progression-free survival (PFS) analysis based on the histological subclassifications. a: Conventional Grade III gliomas (AA, AO, AOA) show significantly longer PFS than Grade IV gliomas (GBM, GBMO). b: A significantly longer PFS in GBMO patients was observed compared to GBM ($p = 0.0456$), while the OS was not significant (Fig. 2b). c: Oligodendroglial tumor ("oligo"; AO, AOA, GBMO) shows significantly longer PFS compared to pure astrocytic tumor ("pure astro"; AA, GBM). d: The PFS curve of AA patients is almost identical to that of GBM patients.
doi:10.1371/journal.pone.0041669.g003

reports [12,13]. Between GBM and GBMO, the statistical significance of OS was not obtained, although the progression-free survival (PFS) of GBMO was statistically better than that of GBM ($p = 0.0456$) (Fig. 2b and 3b). To clarify the prognostic value of the presence of oligodendroglial tumor component, we divided all cases into two groups regardless of WHO grading, i.e., oligodendroglial tumor (AO, AOA, GBMO) and pure astrocytic tumor (AA, GBM), and obtained the interesting result that the both OS and PFS of oligodendroglial tumor were significantly better than these of pure astrocytic tumor (Fig. 2c and 3c). Furthermore, we found the striking data between AA and GBM; their survival curves of the OS and the PFS were almost identical (Fig. 2d, 3d and S3). In our facility, the patients with pathological Grade III glioma (AA, AO and AOA) were treated with a smaller amount of radiation (54 Gy) compared to the patients with Grade IV (GBM and GBMO; 60 Gy), and the selection of chemotherapy varied according to the standard protocol of the time of onset. To exclude the possible effects due to the variation of chemotherapy and the total amount of irradiation, we analyzed the OS between AA and GBM with ACNU, TMZ, or 60 Gy of irradiation, respectively, and confirmed that the OS and PFS were not affected by the variation of the treatment (Fig. 4).

FISH Analysis

Among 18 specimens obtained between 2006 and 2009, nine cases were not applied because of the poor preservation status and/or the shortage of the specimens. Finally, we could detect the signal of fluorescent probe in 9 cases, which include 3 oligodendroglial tumors (3 AOAs) and 6 pure astrocytic tumors (1 AA and 5 GBMs) (Table S1). As a result, four cases showed high percentages (higher than 30%) of 1p36 loss and 5 showed low percentages (less than 30%). Among the 3 oligodendroglial tumors, only 1 case showed positive for 1p36 loss, on the other hand, three cases out of 6 pure astrocytic tumors showed positive for 1p36. There was no significant difference between 1p loss-positive group and 1p loss–negative group with respect to PFS or OS (Figure S2). In order to compare the prognostic significance between 1p loss status and oligodendroglial component, we next divided these 9 patients into oligodendroglial tumors and pure astrocytic tumors and examine the PFS and OS. There was no significant difference between oligodendroglial tumors and pure astrocytic tumors in PFS and OS, however, the each survival curves of oligodendroglial tumors showed distinctly better prognosis than pure astrocytic tumors.

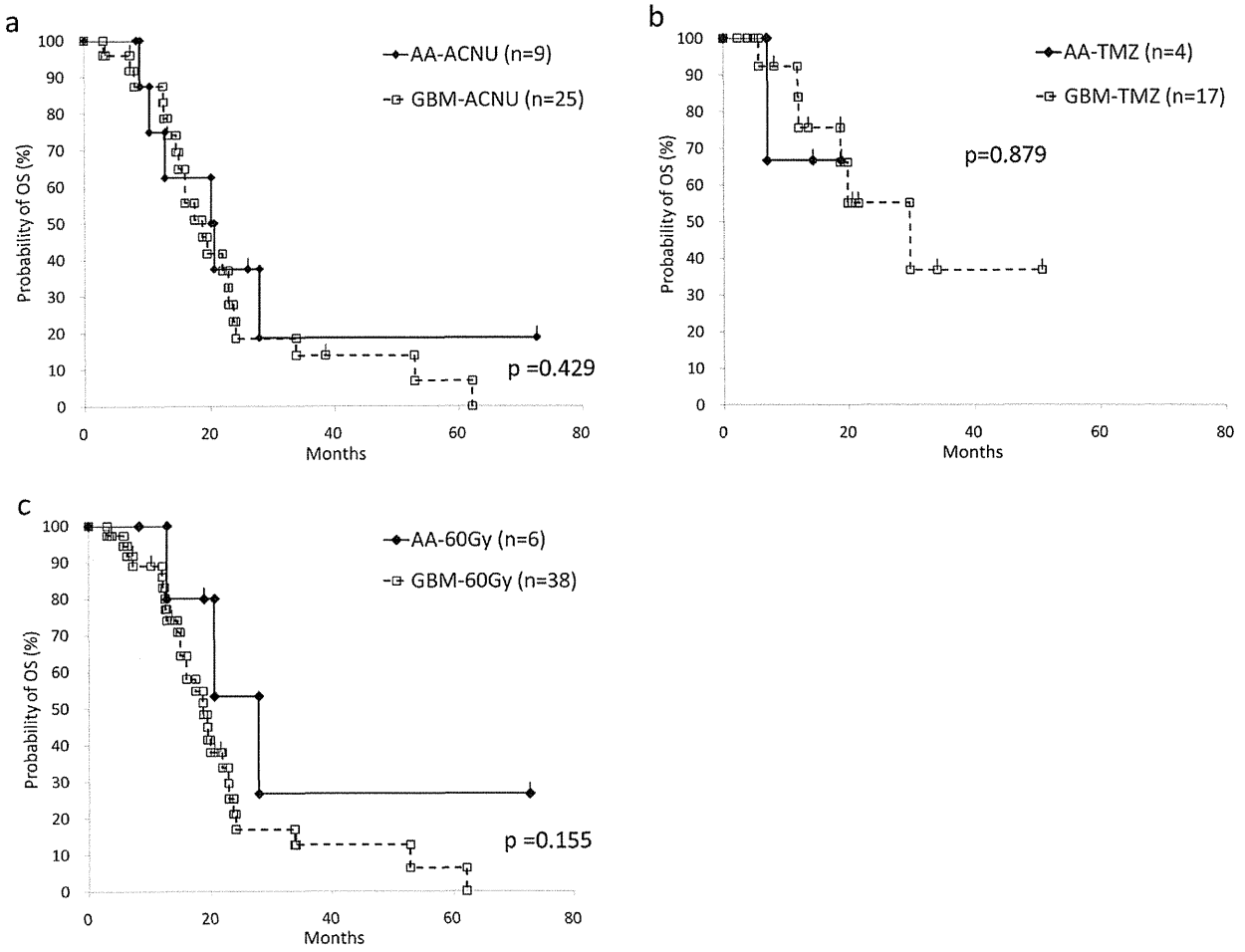

Figure 4. Overall survival analysis of AA and GBM according to the treatment variations. The graph shows comparison of OS between AA and GBM patients who underwent Nimustine hydrochloride (ACNU) - based chemotherapy (a), Temozolomide (TMZ) - based chemotherapy (b), and 60 Gy of radiation therapy (c). There is no statistical siginificance.
doi:10.1371/journal.pone.0041669.g004

Discussion

Because the favorable prognosis of oligodendroglial tumor including AO and AOA has been clinically recognized [1,2,3], the proper pathological diagnosis for these tumors is required. In fact, the recent clinical Phase III trial of anaplastic gliomas revealed that AO and AOA shared the similar prognosis, which was better than that for AA [14]. Regarding GBMO, although its prognostic evaluation still remains controversial [5,6,7,8,9,10], here we have shown that the prognosis of GBMO, at least in terms of PFS, but also in terms of the tendency for OS, was significantly better than that of GBM. In this study, we have performed the alternative categorization of high-grade gliomas throughout Grade III and IV, i.e., into oligodendroglial tumor (AO, AOA and GBMO) and pure astrocytic tumor (AA and GBM), and obtained the notable result of the survival analysis (Fig. 2c and 3c). The survival curves of OS and PFS of the two groups were almost similar to, or much more significant than, that of the conventional categorization into Grade III and IV (Fig. 2a and 3a). Furthermore, the survival analysis within the group of pure astrocytic tumors, more specifically pure astrocytic high grade gliomas, exhibited the unexpected conclusion that the prognosis of AA and GBM was almost identical in OS or even PFS (Fig. 2d and 3d). Based on these results, we concluded that the presence of histological oligodendroglial tumor component, purely or even partially, is a critical prognostic factor for high-grade glioma throughout Grade III and IV, although additional studies to increase the number of the cases for AA (n = 13) which was rather less than that of GBM (n = 57) might be required for further confirmation.

In our histological review process, we defined the oligodendroglial tumor component by identification of the groups of the cells with an obvious perinuclear halo (fried egg appearance) in H&E section; however we did not set the definite numeric value for the proportion of the oligodendroglial tumor component. Establishing the definite criteria for the proportion of oligodendroglial tumor component for diagnosis can be difficult, because the pathological materials obtained by biopsy or even total resection usually reflect the partial aspect of the lesion; in fact, it varied between 10 to 25% in a previous report [1]. The reason that the percentage of GBMO in our series (25%) was higher than previous report (5–20%) [6,7,9] might be explained by such difference of diagnostic criteria for the oligodendroglial tumor component. To distinguish the oligodendroglial tumor from the astrocytic tumor, the immunohistochemical specific marker has not been identified, while the detection of loss of chromosome 1 (1p) and

chromosome 19 (19q) by FISH is established [11,15,16]. However, because the consensus diagnostic criteria of the proportion of cells with 1p and 19q deletion has not been built yet, previous reports indicated the variable cut-off values [17,18,19], and furthermore, FISH technique has not always been one of the routine clinical examinations in general hospitals, and the aged, long term-fixed pathological specimens are sometimes not suitable for this analysis. In fact, we failed the FISH analysis in 9 out of 18 cases because of the poor preservation state and/or the shortage of the specimen. Interestingly, four cases which represented positive for 1p loss included 3 GBMs without histological oligodendroglial tumor component. Moreover, the survival analysis for these 9 cases revealed unexpected results that the histological evaluation for oligodendroglial tumor component was more sensitive factor rather than the FISH analysis for 1p-loss (Figure S2), although it was not statistically significant due to small number of the cases. These results also suggest the diagnostic significance of histological evaluation for oligodendroglial tumor component. In addition, the histological oligodendroglial features including perinuclear halo (classical histology) was noted as a strong predictor of clinical outcome, rather than 1p/19q status [20]. Hence, the fact that the histological identification of the cells with an obvious perinuclear halo (fried egg appearance) in H&E section is enough to discuss the prognosis, as we presented here, is quite important for the majority of the pathologists to make a routine diagnosis and the neurosurgeons to treat the patients with high-grade glioma.

A critical question has arisen: how does the presence of oligodendroglial tumor component, even partially, yield to the favorable prognosis? One of the possible hypotheses is that the cell biology of oligodendroglial tumor would differ from that of astrocytic tumor. The therapeutic sensitivity of 1p/19q-loss oligodendroglioma to chemotherapy and radiation was discussed previously, although it is not clear whether oligodendroglioma represent a tumor type that is more responsive to cytotoxic therapies or whether these tumors are more biologically indolent [15]. The experimental study using oligodendroglial tumor cell line would be expected to answer this query, although there are currently no available cell lines derived from human oligodendroglial tumor.

In conclusion, we emphasize the prognostic significance to identify the oligodendroglial tumor component, even partially, in routine H & E sections of the high-grade gliomas, and would propose the alternative histological grading system of Grade III including GBMO as well as AO and AOA.

Supporting Information

Figure S1 The histological appearance of typical AA (a), AO (b), AOA (c) and GBM (d). a: AA is composed of astrocytic cells with moderate atypia. There is no evident necrosis, prominent vascular proliferation, or oligodendroglial tumor component. b: AO is composed of oligodendrocytic cells with obvious perinuclear halo. c: In AOA, astrocytic cells are intermingled with oligodendrocytic cells. There is no evident necrosis. d: In GBM, diffuse infiltration of pleomorphic tumor cells is observed and the microvascular proliferation is prominent. The foci of necrosis are found in other fields. (The scale bars represent 50 micrometers.).
(TIF)

Figure S2 Survival analysis based on 1p loss status or histological subclassification. The graph shows comparison of progression-free survival (PFS) or overall survival (OS) according to 1p loss status (a, b) and histological subclassification (c, d). Although any of them shows no statistical siginificance between them, oligodendroglial tumor is associated with longer survival.
(TIF)

Figure S3 The overlayed survival curves. The survival curves of the Grade III and oligodendroglial tumor (AO, AOA, GBMO; oligo), and Grade IV and pure astrocytic tumor (AA, GBM; pure astro) were almost identical, respectively.
(TIF)

Table S1 The result of FISH analysis for 1p36 loss. AOA: anaplastic oligoastrocytoma, AA: anaplastic astrocytoma, GBM: glioblastoma, GTR: gross total resection, PR: partial resection, STR: subtotal resection, TMZ: Temozolomide, ACNU: Nimustine hydrochloride, CR: complete response, SD: stable disease, NA: not available, D: death, PFS: progression free survival, OS: overall survival.
(DOCX)

Acknowledgments

We thank Masahito Kato (Hokkaido neurosurgical memorial hospital), Shin Fujimoto (Kashiwaba Neurosurgical Hospital) and Junichi Murata (Sapporo Azabu neurosurgical hospital) for providing clinical data for this analysis.

Author Contributions

Conceived and designed the experiments: HN S. Terasaka. Performed the experiments: HK MT TK S. Tanaka. Analyzed the data: TN. Contributed reagents/materials/analysis tools: SY HK S. Terasaka. Wrote the paper: HK HN.

References

1. Donahue B, Scott CB, Nelson JS, Rotman M, Murray KJ, et al. (1997) Influence of an oligodendroglial component on the survival of patients with anaplastic astrocytomas: a report of Radiation Therapy Oncology Group 83–02. Int J Radiat Oncol Biol Phys 38: 911–914.
2. Shaw EG, Scheithauer BW, O'Fallon JR (1997) Supratentorial gliomas: a comparative study by grade and histologic type. J Neurooncol 31: 273–278.
3. Tortosa A, Vinolas N, Villa S, Verger E, Gil JM, et al. (2003) Prognostic implication of clinical, radiologic, and pathologic features in patients with anaplastic gliomas. Cancer 97: 1063–1071.
4. Louis DN, Ohgaki H, Wiestler OD, Cavenee WK, editors (2007) WHO Classification of Tumours of the Central Nervous System, 4th Edition: IARC Press, Lyons. 164–172 p.
5. Pinto LW, Araujo MB, Vettore AL, Wernersbach L, Leite AC, et al. (2008) Glioblastomas: correlation between oligodendroglial components, genetic abnormalities, and prognosis. Virchows Arch 452: 481–490.
6. Homma T, Fukushima T, Vaccarella S, Yonekawa Y, Di Patre PL, et al. (2006) Correlation among pathology, genotype, and patient outcomes in glioblastoma. J Neuropathol Exp Neurol 65: 846–854.
7. Hilton DA, Penney M, Pobereskin L, Sanders H, Love S (2004) Histological indicators of prognosis in glioblastomas: retinoblastoma protein expression and oligodendroglial differentiation indicate improved survival. Histopathology 44: 555–560.
8. Kraus JA, Lamszus K, Glesmann N, Beck M, Wolter M, et al. (2001) Molecular genetic alterations in glioblastomas with oligodendroglial component. Acta Neuropathol 101: 311–320.
9. Salvati M, Formichella AI, D'Elia A, Brogna C, Frati A, et al. (2009) Cerebral glioblastoma with oligodendroglioma component: analysis of 36 cases. J Neurooncol 94: 129–134.
10. Miller CR, Dunham CP, Scheithauer BW, Perry A (2006) Significance of necrosis in grading of oligodendroglial neoplasms: a clinicopathologic and genetic study of newly diagnosed high-grade gliomas. J Clin Oncol 24: 5419–5426.
11. Burger PC, Minn AY, Smith JS, Borell TJ, Jedlicka AE, et al. (2001) Losses of chromosomal arms 1p and 19q in the diagnosis of oligodendroglioma. A study of paraffin-embedded sections. Mod Pathol 14: 842–853.

12. Laws ER, Parney IF, Huang W, Anderson F, Morris AM, et al. (2003) Survival following surgery and prognostic factors for recently diagnosed malignant glioma: data from the Glioma Outcomes Project. J Neurosurg 99: 467–473.
13. Salminen E, Nuutinen JM, Huhtala S (1996) Multivariate analysis of prognostic factors in 106 patients with malignant glioma. Eur J Cancer 32A: 1918–1923.
14. Wick W, Hartmann C, Engel C, Stoffels M, Felsberg J, et al. (2009) NOA-04 randomized phase III trial of sequential radiochemotherapy of anaplastic glioma with procarbazine, lomustine, and vincristine or temozolomide. J Clin Oncol 27: 5874–5880.
15. Aldape K, Burger PC, Perry A (2007) Clinicopathologic aspects of 1p/19q loss and the diagnosis of oligodendroglioma. Arch Pathol Lab Med 131: 242–251.
16. Hartmann C, Mueller W, von Deimling A (2004) Pathology and molecular genetics of oligodendroglial tumors. J Mol Med 82: 638–655.
17. van den Bent MJ, Carpentier AF, Brandes AA, Sanson M, Taphoorn MJ, et al. (2006) Adjuvant procarbazine, lomustine, and vincristine improves progression-free survival but not overall survival in newly diagnosed anaplastic oligodendrogliomas and oligoastrocytomas: a randomized European Organisation for Research and Treatment of Cancer phase III trial. J Clin Oncol 24: 2715–2722.
18. Smith JS, Perry A, Borell TJ, Lee HK, O'Fallon J, et al. (2000) Alterations of chromosome arms 1p and 19q as predictors of survival in oligodendrogliomas, astrocytomas, and mixed oligoastrocytomas. J Clin Oncol 18: 636–645.
19. Fuller CE, Schmidt RE, Roth KA, Burger PC, Scheithauer BW, et al. (2003) Clinical utility of fluorescence in situ hybridization (FISH) in morphologically ambiguous gliomas with hybrid oligodendroglial/astrocytic features. J Neuropathol Exp Neurol 62: 1118–1128.
20. McDonald JM, See SJ, Tremont IW, Colman H, Gilbert MR, et al. (2005) The prognostic impact of histology and 1p/19q status in anaplastic oligodendroglial tumors. Cancer 104: 1468–1477.

Increased Adenosine A_1 Receptor Levels in Hemianopia Patients After Cerebral Injury

An Application of PET Using ^{11}C-8-Dicyclopropylmethyl-1-Methyl-3-Propylxanthine

Yukihisa Suzuki, MD, PhD,‡ Tadashi Nariai, MD, PhD,†‡ Motohiro Kiyosawa, MD, PhD,*‡ Manabu Mochizuki, MD, PhD,* Yuichi Kimura, PhD,‡§ Keiichi Oda, PhD,‡ Kenji Ishii, MD,‡ and Kiich Ishiwata, PhD‡*

Purpose: The aim of this study was to apply positron emission tomography (PET) with ^{11}C-8-dicyclopropylmethyl-1-methyl-3-propylxanthine (MPDX), a radioligand for adenosine A_1 receptor (A1R), to patients with hemianopia caused by brain injury to study neurorepair mechanisms in the brain.

Patients and Methods: Four patients with homonymous hemianopia and 15 healthy subjects were examined using PET to measure cerebral glucose metabolism, ^{11}C-flumazenil (FMZ) binding to the central benzodiazepine receptor, and MPDX binding to A1R. Left and right regions of interest (ROIs) were selected, and semiquantitative data on the 3 kinds of PET examinations were obtained. The ROIs were referenced using the data for homologous regions in the contralateral hemisphere [ipsilateral/contralateral (I/C) ratio].

Results: The I/C ratios for cerebral glucose metabolism and FMZ binding were low in the primary visual cortex (PVC) and visual association cortex in all the patients, whereas MPDX binding increased in the PVC in patients 1 and 2. Patients 1 and 2 experienced improvement in their visual field after 1 year. However, the other 2 patients showed no changes. We observed an increase in MPDX binding to A1R in the injured portion of the PVC in the patients who recovered.

Conclusions: Evaluation of A1R by MPDX-PET may be useful for predicting prognosis and understanding the compensatory and reorganization processes in hemianopia caused by organic brain damage.

Key Words: adenosine A_1 receptor, homonymous hemianopia, neurorepair mechanisms, positron emission tomography, primary visual cortex, visual field

(*Clin Nucl Med* 2012;37: 1146–1151)

Adenosine is an endogenous modulator of the brain and seems to have a net inhibitory effect on neuronal tissues. Adenosine receptors play roles in neurological and psychiatric disorders, such as Alzheimer disease, Parkinson disease, epilepsy, and schizophrenia. Therefore, adenosine receptors are interesting targets of positron emission tomography (PET) for understanding the mechanisms underlying the pathogenesis of diseases and developing new therapeutics.[1–3] We developed ^{11}C-8-dicyclopropylmethyl-1-methyl-3-propylxanthine (MPDX) and ^{11}C-(*E*)-8-(3,4,5-trimethoxystyryl)-1,3,7-trimethylxanthine for mapping adenosine A_1 receptor (A1R) and A_{2A} receptor, respectively[4]; so far, both have been applied to Alzheimer and Parkinson diseases, respectively.[5,6] MPDX-PET was also applied preliminarily to patients with temporal lobe epilepsy.[4] In their experimental studies, Nariai et al[7] demonstrated that the reduction of MPDX binding is more severe than those of glucose metabolism and ^{11}C-flumazenil (FMZ) binding to the central benzodiazepine receptor (cBZR) in an ischemic cat model. This suggests that MPDX-PET is preferable over ^{18}F-fluorodeoxyglucose (FDG)-PET and FMZ-PET for the prediction of ischemic insults. Kiyosawa et al[8,9] performed ex vivo autoradiography of a monocularly enucleated rat brain using MPDX and FMZ; they found that axon degeneration resulted in presynaptic A1R loss and a transient upregulation of postsynaptic cBZR density in the superior colliculus. However, the changes occurring in adenosine receptors after brain ischemia or injury in humans remain unclear.

In the present study, we evaluated cerebral glucose metabolism, and FMZ and MPDX binding in 4 patients with hemianopia caused by cerebral injury. Because patients in whom only the visual cortex is selectively injured are very rare,[10] it was difficult to recruit many patients to participate in this study. Nonetheless, we found novel and useful information regarding MPDX-PET in patients with organic brain damage.

Regarding the visual cortex, damage produces homonymous visual field defects contralateral to the side of the lesion. In most cases, in clinical practice, visual field defects improve gradually over several months. Experimental research shows that mature central nervous systems have a certain capacity to undergo repair and reorganization after injury.

Diffusion-weighted MRI or FDG-PET has been used to evaluate acute ischemic cerebral lesions.[11,12] Moreover, Heiss et al[13] evaluated ischemic cortical damages using FMZ-PET in acute stroke patients. Recently, we reported the role of FMZ-PET in predicting long-term prognosis of hemianopia caused by organic brain damage.[4]

PATIENTS AND METHODS

We studied 4 patients (3 men and 1 woman; age, 34–73 years) with homonymous visual field defects caused by ischemic lesions or tumors of the posterior afferent visual system. We excluded patients in whom the bilateral visual cortex or other areas in the brain were injured. All the patients had a corrected visual acuity of 20/20 in both eyes, and clinical examination of the fundi revealed no defects. Their eye movements were full and smooth. A total of 15 healthy individuals, including 6 men and 9 women (age, 54.3 ± 4.4 years), volunteered to be in the control group. All the subjects underwent MRI and PET with FDG, FMZ, and MPDX.

Informed consent was obtained from all the subjects before their participation in the PET study. The study protocol was approved by the institutional ethics committee of Tokyo Metropolitan Institute of Gerontology. All the procedures conformed to the tenets of the Declaration of Helsinki.

MRI Scanning

The MRI scans were obtained for all the subjects by using a 1.5-T Signa Horizon scanner (General Electric, Milwaukee, WI). Transaxial

Received for publication February 4, 2012; revision accepted May 15, 2012.
From the *Department of Ophthalmology and Visual Science and †Department of Neurosurgery, Tokyo Medical and Dental University, Graduate School, Tokyo; ‡Positron Medical Center, Tokyo Metropolitan Institute of Gerontology, Tokyo; and §Molecular Imaging Center, National Institute of Radiological Sciences, Chiba, Japan.
Conflicts of interest and sources of funding: none declared.
This research was performed at the Positron Medical Center, Tokyo Metropolitan Institute of Gerontology.
Reprints: Yukihisa Suzuki, MD, PhD, Department of Ophthalmology and Visual Science, Tokyo Medical and Dental University, Graduate School, Yushima 1 chome-5-45, Bunkyo-ku, Tokyo 113-8519, Japan.
E-mail: suzuki@f8.dion.ne.jp.

ISSN: 0363-9762/12/3712–1146

images were obtained with T1-weighted contrast [3D-spoiled gradient echo (3D-SPGR), TR = 9.2 ms, echo time (TE) = 2.0 ms, matrix size = 256 × 256 × 124, and voxel size = 0.94 × 0.94 × 1.3 mm], T2-weighted contrast (first spin echo, TR = 3000 ms, TE = 100 ms, matrix size = 256 × 256 × 20, and voxel size = 0.7 × 0.7 × 6.5 mm), and fluid-attenuated inversion recovery [TR = 10,002 ms, TE = 106.5 ms, inversion time (TI) = 2500 ms, matrix size = 256 × 256 × 19, and voxel size = 0.86 × 0.86 × 5 mm] imaging techniques.

PET Data Acquisition

The PET scans were obtained using the SET 2400W scanner (Shimadzu, Kyoto, Japan) at the Positron Medical Center, Tokyo Metropolitan Institute of Gerontology.

For the FDG-PET scan, a bolus of 2.5-MBq/kg (body weight) FDG was injected intravenously. Each subject was instructed to lie down with their eyes closed during the accumulation time. A 6-minute emission scan in the 3-dimensional acquisition mode was initiated 45 minutes after the injection of FDG, and 50 transaxial images with an interslice interval of 3.125 mm were obtained (matrix size = 128 × 128 × 63 and voxel size = 2.0 × 2.0 × 3.125 mm). The tomographic images were reconstructed using the filtered back-projection method using a Butterworth filter (cut-off frequency, 1.25 cycles/cm; order, 2). A standardized uptake value [SUV, (activity/mL tissue)/(injected activity/g of body weight)] image was considered to reflect the regional cerebral glucose metabolism.

For the FMZ-PET scan, a bolus of 6.0-MBq/kg (body weight) FMZ was injected intravenously, and the FMZ binding data were acquired in the 3-dimensional mode of static scanning (matrix size = 128× 128 × 63 and voxel size = 2.0 × 2.0 × 3.125 mm) from 20 to 40 minutes after FMZ injection as described previously.[14] The specific activity and amount of injected cold material were 58.3 ± 64.6 MBq/nmol and 12.1 ± 8.6 nmol, respectively. A 20-minute emission scan was initiated 20 minutes after the FMZ injection; this time window image exhibited the strongest correlation with the distribution volume image based on the dynamic date with arterial blood sampling[14] and was considered to reflect the FMZ-binding capacity.

For the MPDX-PET scan, a bolus of 8.0-MBq/kg (body weight) MPDX was injected intravenously, and a dynamic PET scan was performed in the 2-dimensional mode (matrix size = 128 × 128 × 31 and voxel size = 2.0 × 2.0 × 6.25 mm) as described previously.[5,15] The specific activity and amount of injected cold material were 79.4 ± 40.8 MBq/nmol and 10.1 ± 12.8 nmol, respectively. Serial arterial blood samples were obtained via a catheter inserted into the radial artery, and plasma radioactivity and metabolites were measured. A 60-minute dynamic emission scan was initiated upon MPDX injection. The binding potential of MPDX was evaluated on the basis of the Logan graphical analysis with arterial input using the cerebellum as a reference region.[15,16]

In each PET scan, attenuation was corrected by performing a transmission scan using a rotating $^{68}Ga/^{68}Ge$ source.

Data Processing

The PET images were registered in the 3-dimensional mode to the individual 3D-SPGR MRIs by using the Automated Medical Images Registration (AMIR) program.[17] Further data analysis was performed using Dr. View software (AJS, Tokyo, Japan). Regions of interest (ROIs), that is, circles with an 8-mm diameter, were interactively defined on the 3D-SPGR MRIs by visual observation with reference to the coregistered PET images. Bilateral ROIs were selected in the primary visual cortex (PVC), visual association cortex (VAC), cuneus, thalamus, caudate nucleus, putamen, and insula, and cerebral glucose metabolism; in addition, the FMZ and MPDX binding in these regions were measured (Fig. 1). These 3 parameters recorded for each ROI were compared with those recorded for the homologous regions in the contralateral hemisphere by calculating the ipsilateral/contralateral (I/C) ratio.[18] By calculating the I/C ratios from the SUVs for FDG and FMZ and those from the binding potential for MPDX, the values are the same as the corresponding values of the quantitative images. In the group analysis, the differences in I/C ratios between the patient and control groups were tested using the Mann-Whitney U test with a Bonferroni's correction for multiple comparisons ($P < 0.007 = 0.05/7$). During the individual analyses, we defined a significant change in the I/C ratio in each patient as an increase or decrease over the normal mean ± 2 SDs. One year after the onset of hemianopia, Goldmann perimetry was performed again.

RESULTS

Case Presentations

Patient 1

A 73-year-old right-handed man underwent a lobectomy because of left lateral lung cancer. The MRI performed after 10 months revealed a solitary metastatic tumor in the right occipital cortex, and the patient received another operation to resect the brain tumor. Goldmann visual fields detected left homonymous hemianopia. We ordered FDG-PET, FMZ-PET, and MPDX-PET scanning 1 month later.

Patient 2

A 34-year-old right-handed woman was under observation for moyamoya disease. She experienced a left visual field defect but

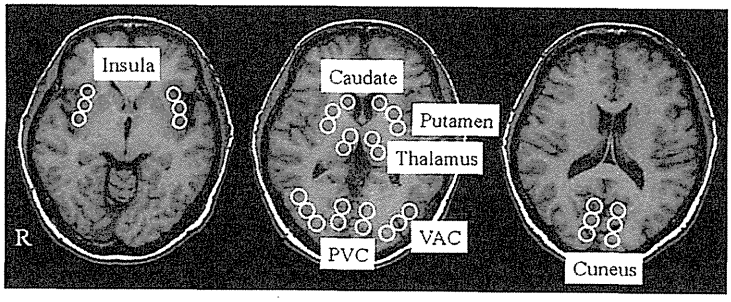

FIGURE 1. Structures on which regions of interest were placed included the primary visual cortex (PVC), visual association cortex (VAC), cuneus, thalamus, caudate, putamen, and insula.

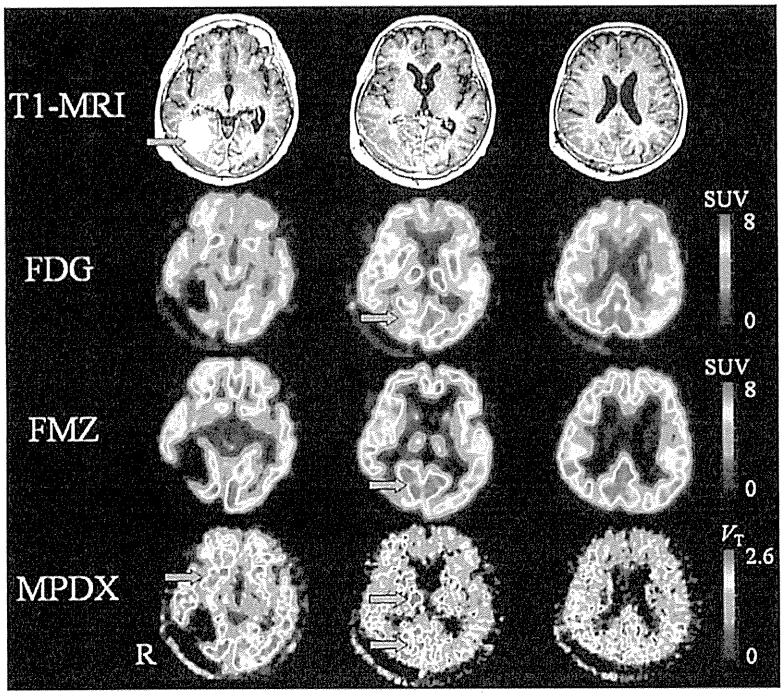

FIGURE 2. T1-weighted magnetic resonance images (MRI; top) and positron emission tomographic (PET) images with ^{18}F-fluorodeoxyglucose (FDG; second line), ^{11}C-flumazenil (FMZ; third line), and ^{11}C-8-dicyclopropylmethyl-1-methyl-3-propylxanthine (MPDX; bottom) in patient 1. The FDG and FMZ images were standardized uptake value [SUV, (activity/mL tissue)/(injected activity/g of body weight)] images, and the MPDX image was a distribution volume (mL/mL) image. The PET images for FDG, FMZ, and MPDX were acquired from 45 to 51, 20 to 40, and 0 to 60 min after the injection, respectively. There was a tumor in the right lingual gyrus (green arrow). Glucose metabolism and FMZ binding in the right primary visual cortex (PVC) decreased (gray arrows); however, FMZ binding increased in the right cuneus, and MPDX binding increased in the right PVC (pink arrow), cuneus, thalamus, and insula.

no symptoms until that time. Magnetic resonance angiography revealed an occlusion of the right posterior cerebral artery. Goldmann visual fields detected left homonymous hemianopia. We ordered MRI and 3 kinds of PET scans 1 month later.

Patient 3

A 71-year-old right-handed man without any history of serious illness experienced numbness in his lip. After 2 days, he visited the hospital because of right lateral numbness. MRI revealed infarctions in the left PVC and injury in the left optic radiation. Goldmann visual fields revealed right homonymous hemianopia. We ordered FDG-PET and FMZ-PET scanning 3 months later and MPDX-PET scanning 5 months later.

Patient 4

A 56-year-old right-handed man had no history of serious illness. He visited the hospital because of a sudden onset of speech disturbance. Aphasia, right hemispatial neglect, and right hemiparesis were observed. CT scanning revealed a hematoma in the left temporal lobe. The hematoma was surgically removed on the same day. Goldmann visual fields revealed right homonymous hemianopia. We performed MRI and 3 kinds of PET scans 7 months later.

One year after the onset, the visual field defect improved in patients 1 and 2 (recovered patients) but not in patients 3 or 4 (unchanged patients). The typical SUV images of FDG-PET and FMZ-PET and a binding potential image of MPDX-PET are shown in Figure 2. The I/C ratios for cerebral glucose metabolism and FMZ binding in the PVC and VAC decreased in the patient group ($P < 0.05$; Tables 1 and 2). The ratio of MPDX binding in the PVC increased in the recovered patients but decreased in the unchanged patients (Table 3). The I/C ratio for FMZ binding in the cuneus increased in the patient group ($P < 0.05$; Table 2), whereas that of glucose metabolism decreased in 3 patients (Table 1). Moreover, the I/C ratios for MPDX binding in the thalamus and insula increased in 2 and 1 patient, respectively.

DISCUSSION

Adenosine is an endogenous modulator of brain functioning, and adenosine receptors play roles in neurological and psychiatric disorders.[1–6] Several experimental studies suggest that changes in the adenosine receptors occur after brain ischemia or injury and that adenosine receptors are associated with neurorepair mechanisms, such as visual reorganization.[7,9] However, PET studies on these receptors in the human brain are limited. In the present study, we evaluated A1R-MPDX binding, cerebral glucose metabolism, and FMZ binding in 4 patients with hemianopia caused by cerebral injury. Because patients

TABLE 1. Ipsilateral/Contralateral (I/C) Ratio for Cerebral Glucose Metabolism in the Brain of Hemianopia Patients

		Area						
Patient	Term	PVC	VAC	Cuneus	Thalamus	Caudate	Putamen	Insula
1	1M	0.832*	0.812*	1.003	0.964*	1.029	0.961	0.992
2	1M	0.809*	0.770*	0.830*	0.989	0.975	0.929*	0.995
3	3M	0.550*	0.706*	0.828*	0.981	0.981	0.998	0.978
4	7M	0.642*	0.846*	0.833*	1.006	0.902*	0.998	0.917
Average of patients		0.708† ± 0.135	0.784† ± 0.060	0.874 ± 0.086	0.985 ± 0.017	0.972 ± 0.052	0.972 ± 0.033	0.971 ± 0.036
Average of normal subjects		0.996 ± 0.026	1.008 ± 0.027	0.996 ± 0.036	1.004 ± 0.020	1.002 ± 0.028	1.000 ± 0.032	0.980 ± 0.052

*Significant decrease in the I/C ratio (below the normal average − 2 SD).
†Significant decrease in the I/C ratio (Mann–Whitney U test with multiple comparison, $P < 0.05$).
PVC indicates primary visual cortex; VAC, visual association cortex.

with a selectively injured visual cortex are very rare,[10] there are drawbacks in a small sample size and subject population. Therefore, the present study is a hypothesis-generating study suggesting that MPDX-PET is a useful tool for estimating the degree of brain damage and predicting the prognosis. Meanwhile, FDG- and FMZ-PET have already been established for the study of various brain disorders.[10–13] Further larger studies are needed to confirm the novel and useful findings of MPDX-PET in patients with organic brain damage.

Regarding subject populations, the sex ratios and ages differed between the patients and healthy controls. However, we suspect that age and sex hardly affected the results of the present study because we presented the results using the I/C ratios normalized to the values of homologous regions in the contralateral hemisphere in each patient. When referring to previous reports on aging and sex effects on A1R, cBZR, and glucose metabolism, Meyer et al[10] observed no significant effect of sex on human cerebral A1R binding using PET or [^{18}F]CPFPX, another A1R ligand with the same xanthine structure. In addition, they did not observe any significant associations between age and the total distribution volume in any region, but found a significant negative correlation between age and binding potential in all cerebral regions except the cingulate gyrus. Moreover, no aging and sex effects in human cBZR binding were reported.[20,21] Meanwhile, there are several reports on age- or sex-related changes in cerebral glucose metabolism using FDG-PET. For example, Fujimoto et al[22] observed age-related increases in subjects 20–50 years old and decreases in subjects 50–80 years old in the parahippocampal and amygdala regions, as well as age-related decreases in the frontal lobe from 20 to 50 years old. Kawachi et al[23] observed that men have significantly higher glucose metabolism in the right insula, middle temporal gyrus, and medial frontal lobe than women; meanwhile, glucose metabolism in the hypothalamus is significantly higher in women than in men.

Cerebral Glucose Metabolism and FMZ Binding in the Hemianopia Patients

A previous PET study[11] reports that in the hemianopia patients, cerebral glucose metabolism increases after ischemic lesions and is accompanied by recovery of the visual field. Even if neurons survive in the area of injury, glucose hypometabolism is usually observed in this area because of diaschisis in the early stage of onset. Because glucose metabolism in the areas affected by diaschisis may subsequently improve, it is difficult to determine the density of surviving neurons in the areas of injury using only the early FDG-PET findings.

On the other hand, FMZ binding in the injured areas reflects the number of surviving neurons, even during the early stage of onset.[13] We found that patients with high FMZ binding in the PVC can be expected to recover their visual field. The I/C ratio for FMZ binding in the PVC and recovery of the visual field are thought to be correlated.[18] The I/C ratio for FMZ binding increased in the cuneus in the patients. Adenosine content increases in ischemic conditions,[24] and stimulation of A1R decreases spontaneous gamma-amino-butyric

TABLE 2. Ipsilateral/Contralateral (I/C) Ratio for FMZ Binding in the Brain of Hemianopia Patients

		Area						
Patient	Term	PVC	VAC	Cuneus	Thalamus	Caudate	Putamen	Insula
1	1M	0.914†	0.765†	1.116*	0.996	1.002	0.922	0.988
2	1M	0.913†	0.990	1.071*	0.930	0.977	0.963	0.989
3	3M	0.807†	0.923†	1.029*	0.998	1.062	1.021	0.999
4	7M	0.790†	0.786†	1.035*	1.015	0.828†	0.901	0.978†
Average of patients		0.856§ ± 0.067	0.866§ ± 0.108	1.063‡ ± 0.040	0.985 ± 0.037	0.967 ± 0.099	0.952 ± 0.053	0.989 ± 0.009
Average of normal subjects		0.997 ± 0.015	1.006 ± 0.024	1.000 ± 0.003	0.991 ± 0.052	1.004 ± 0.031	1.011 ± 0.088	1.004 ± 0.009

*Significant increase in the I/C ratio (over the normal average + 2 SD).
†Significant decrease in the I/C ratio (below the normal average − 2 SD).
‡Significant increase in the I/C ratio (Mann–Whitney U test, $P < 0.05$).
§Significant decrease in the I/C ratio (Mann–Whitney U test, $P < 0.05$).
PVC indicates primary visual cortex; VAC, visual association cortex.

TABLE 3. Ipsilateral/Contralateral (I/C) Ratio for MPDX Binding in the Brain of Hemianopia Patients

		Area						
Patient	Term	PVC	VAC	Cuneus	Thalamus	Caudate	Putamen	Insula
1	1M	1.084*	0.932	0.999	1.072*	0.962	1.039	1.077*
2	1M	1.065*	0.985	0.997	1.012	0.991	0.945	1.034
3	5M	0.840†	0.971	0.969	0.873†	0.905	0.971	0.959
4	7M	0.968	0.946	0.983	1.104*	1.074	0.928†	0.914
Average of patients		0.989 + 0.112	0.959 + 0.024	0.987 + 0.014	1.015 + 0.102	0.983 + 0.070	0.971 + 0.049	0.996 + 0.074
Average of normal subjects		0.987 + 0.038	0.982 + 0.025	1.000 + 0.034	0.999 + 0.027	1.001 + 0.049	1.000 + 0.032	0.988 ± 0.043

*Significant increase in the I/C ratio (over the normal average + 2 SD).
†Significant decrease in the I/C ratio (below the normal average − 2 SD).
PVC indicates primary visual cortex; VAC, visual association cortex.

acid (GABA) release.[25,26] Following the decrease in GABA levels, the density of cBZR, the postsynaptic $GABA_A$ receptor, may be increased as a result of upregulation.[18]

MPDX Binding in the Hemianopia Patients

We observed that the I/C ratio for MPDX binding increased in the PVC and the surrounding and distant areas (ie, the thalamus in 2 patients and the insula in 1 patient) in the recovered patients. Several reports suggest that the quantity and/or binding affinity of A1R increases after ischemia. Lai et al[27] studied the mRNA and protein levels of A1R in the cerebral cortical tissues of rats after ischemia induced by ligation of the common carotid arteries. They observed that the mRNA and protein levels of A1R increased significantly in ischemic tissues compared with those in healthy controls. Moreover, Siniscalchi et al[28] studied A1R binding in the rat cerebral cortex after ischemia and found that the binding capacity and affinity of A1R increased.

A1R in the central nervous system is present presynaptically and postsynaptically; furthermore, in addition to the postsynaptic condition, MPDX reflects the presynaptic condition as well.[29] The critical role of the A1R in the attenuation of brain damage after ischemia is well established. Many studies report that in ischemia, treatment with A1R agonists attenuates the damage in brain tissues and neurons. Action mechanisms triggered by A1R activation play roles in several pathways; these mechanisms include the reduction of metabolic damage caused by hypoxia or glucose–oxygen deprivation,[30] preservation of microtubule-associated protein 2[31]; decrease in excitatory amino acid release and/or synaptic transmission,[32] and inhibition of Ca^{2+} uptake.[33] On the other hand, neuronal cells in the ischemic core induce necrosis, whereas apoptosis delays infarct and retards the border zone in the ischemic tissue.[34] D'Alimonte et al[35] reported that apoptosis in astrocytes was prevented by A1R activation in a rat model. A1R activation produces preconditioning to protect the heart and other tissues from subsequent ischemic injury.[36] Elevated A1R activity may play a protective role in damaged tissues.

We observed that the I/C ratio for MPDX binding increased in the PVC in recovered patients, whereas it was low in the unchanged patients. Nariai et al[7] examined MPDX binding using PET in an occlusion and reperfusion model of the cat middle cerebral artery. They divided the cats into 3 groups: the first group died on the first day because of severe conditions, the second group survived and had infarcted lesions in the cortex and striatum, and the third group survived and had infarcted lesions only in the striatum. They observed that MPDX binding was significantly lower in the first group than the second and third groups, whereas there was no difference between the second group and the healthy controls. We suggest 2 possible reasons why MPDX binding decreased in the severely ischemic regions. First, the number of intact neurons decreased in the severely ischemic regions because low FMZ binding was observed in the unchanged patients. Second, the rate of MPDX binding to A1R might have decreased in the severe ischemic area. Ischemic conditions induce marked elevation of extracellular adenosine levels.[24] In this condition, competition between intrinsic adenosine and an extrinsically injected tracer might decrease the binding of MPDX to A1R.[7] Therefore, MPDX binding in the injured area may reflect the degree of damage.

All of the above-mentioned reports concern the acute stage. One study reported that the upregulation of A1R in lesions increased until 7 days after cerebral ischemia in rats and that A1Rs in lesions tended to decrease at this time.[37] Although there are no previous reports on the changes in A1R binding in the chronic phase, the results of Zhou et al[37] suggest that A1R binding is lower in the chronic phase than in the acute stage.

CONCLUSIONS

We examined MPDX binding to A1R in the brains of patients with hemianopia caused by organic brain damage in the chronic phase. The MPDX binding in the injured side in the PVC was elevated in the recovered patients but remained low in the unchanged patients. Evaluating A1R using MPDX-PET may be useful for estimating the degree of brain damage and predicting prognosis.

ACKNOWLEDGMENTS

Grants: This research was supported by Grants-in-Aid for Scientific Research (B) nos. 21791725 (Y.S.), (B) 16390348 (Ki.I.), and (B) 20390334 (Ki.I.) from the Japan Society for the Promotion of Science.

REFERENCES

1. Ishiwata K, Shimada J, Ishii K, et al. Assessment of adenosine A2A receptors with PET as a new diagnostic tool for neurological disorders. *Drugs Future*. 2002;27:569–576.
2. Ishiwata K, Kimura Y, de Vries EFJ, et al. PET tracers for mapping adenosine receptors as probes for diagnosis of CNS disorders. *Cent Nerv Syst Agents Med Chem*. 2007;7:57–77.
3. Bauer A, Ishiwata K. Adenosine receptor ligands and PET imaging of the CNS. *Handb Exp Pharmacol*. 2009;193:617–642.
4. Ishiwata K, Kimura Y, Oda K, et al. Development of PET radiopharmaceuticals and their clinical applications at the Positron Medical Center. *Geriatr Gerontol Int*. 2010;10(suppl 1):S180–S196.
5. Fukumitsu N, Ishii K, Kimura Y, et al. Adenosine A1 receptors using 8-dicyclopropylmethyl-1-[^{11}C]-methyl-3-propylxanthine PET in Alzheimer's disease. *Ann Nucl Med*. 2008;22:841–847.

6. Mishina M, Ishiwata K, Naganawa M, et al. Adenosine A2A receptors measured with [^{11}C]TMSX PET in the striata of Parkinson's disease patients. *PLoS ONE*. 2011;6:e17338.
7. Nariai T, Shimada Y, Ishiwata K, et al. PET imaging of adenosine A1 receptors with ^{11}C-MPDX as an indicator of severe cerebral ischemic insult. *J Nucl Med*. 2003;44:1839–1844.
8. Kiyosawa M, Ishiwata K, Noguchi J, et al. Neuroreceptor bindings and synaptic activity in visual system of monocularly enucleated rat. *Jpn J Ophthalmol*. 2001; 45:264–269.
9. Wang WF, Ishiwata K, Kiyosawa M, et al. Adenosine A1 and benzodiazepine receptors and glucose metabolism in the visual structures of rats monocularly deprivated by enucleation or eyelid suture at a sensitive period. *Jpn J Ophthalmol*. 2003;47:182–190.
10. Suzuki Y, Kiyosawa M, Mochizuki M, et al. Cortical blindness following aortic arch surgery. *Jpn J Ophthalmol*. 2001;45:547–549.
11. Bosley TM, Dann R, Silver FL, et al. Recovery of vision after ischemic lesions: positron emission tomography. *Ann Neurol*. 1987;21:444–450.
12. Heiss WD, Sobesky J, Smekal U, et al. Probability of cortical infarction predicted by flumazenil binding and diffusion-weighted imaging signal intensity: a comparative positron emission tomography/magnetic resonance imaging study in early ischemic stroke. *Stroke*. 2004;35:1892–1898.
13. Heiss WD, Kracht L, Grond M, et al. Early [^{11}C]-flumazenil/H_2O positron emission tomography predicts irreversible ischemic cortical damage in stroke patients receiving acute thrombolytic therapy. *Stroke*. 2000;31:366–369.
14. Mishina M, Senda M, Kimura Y, et al. Intrasubject correlation between static scan and distribution volume images for [^{11}C]flumazenil PET. *Ann Nucl Med*. 2000;14:193–198.
15. Kimura Y, Ishii K, Fukumitsu N, et al. Quantitative analysis of adenosine A1 receptors in human brain using positron emission tomography and [1-methyl-^{11}C]8-dicyclopropylmethyl-1-methyl-3-propylxanthine. *Nucl Med Biol*. 2004;31: 975–981.
16. Logan J, Fowler JS, Volkow ND, et al. Graphical analysis of reversible radioligand binding from time–activity measurements applied to [N-^{11}C-methyl]-(−)-cocaine PET studies in human subjects. *J Cereb Blood Flow Metab*. 1990;10: 740–747.
17. Ardekani BA, Braun M. A fully automatic multimodality image registration algorithm. *J Comput Assist Tomogr*. 1995;19:615–623.
18. Suzuki Y, Horie C, Kiyosawa M, et al. Measurement of ^{11}C-flumazenil binding in the visual cortex predicts the prognosis of hemianopia. *J Neurol Sci*. 2008; 268:102–107.
19. Meyer PT, Elmenhorst D, Boy C, et al. Effect of aging on cerebral A1 adenosine receptors: a [^{18}F]CPFPX PET study in humans. *Neurobiol Aging*. 2007;28: 1914–1924.
20. Suhara T, Inoue O, Kobayashi K, et al. No age-related changes in human benzodiazepine receptor binding measured by PET with [^{11}C]Ro 15-4513. *Neurosci Lett*. 1993;159:207–210.
21. Zezula J, Cortés R, Probst A, et al. Benzodiazepine receptor sites in the human brain: autoradiographic mapping. *Neuroscience*. 1988;25:771–795.
22. Fujimoto T, Matsumoto T, Fujita S, et al. Changes in glucose metabolism due to aging and gender-related differences in the healthy human brain. *Psychiatry Res*. 2008;164:58–72.
23. Kawachi T, Ishii K, Sakamoto S, et al. Gender differences in cerebral glucose metabolism: a PET study. *J Neurol Sci*. 2002;199:79–83.
24. Hagberg H, Anderson P, Lacarewicz J, et al. Extracellular adenosine, inosine, hypoxanthine, and xanthine in relation to tissue nucleotides and purines in rat striatum during transient ischemia. *J Neurochem*. 1987;49:227–231.
25. Mayfield RD, Jones BA, Miller HA, et al. Modulation of endogenous GABA release by an antagonistic adenosine A1/dopamine D1 receptor interaction in rat brain limbic regions but not basal ganglia. *Synapse*. 1999;33:274–281.
26. Jeong HJ, Jang IS, Nabekura J, et al. Adenosine A1 receptor-mediated presynaptic inhibition of GABAergic transmission in immature rat hippocampal CA1 neurons. *J Neurophysiol*. 2003;89:1214–1222.
27. Lai DM, Tu YK, Liu IM, et al. Increase of adenosine A1 receptor gene expression in cerebral ischemia of Wistar rats. *Neurosci Lett*. 2005;387:59–61.
28. Siniscalchi A, Rodi D, Gessi S, et al. Early changes in adenosine A1 receptors in cerebral cortex slices submitted to in vitro ischemia. *Neurochem Int*. 1999;34: 517–522.
29. Ishiwata K, Nariai T, Kimura Y, et al. Preclinical studies on [^{11}C]MPDX for mapping adenosine A1 receptors by positron emission tomography. *Ann Nucl Med*. 2002;16:377–382.
30. Logan M, Sweeney MI. Adenosine A1 receptor activation preferentially protects cultured cerebellar neurons versus astrocytes against hypoxia-induced death. *Mol Chem Neuropathol*. 1997;31:119–133.
31. Von Lubitz DK, Lin RC, Paul LA, et al. Postischemic administration of adenosine amine congener (ADAC): analysis of recovery in gerbils. *Eur J Pharmacol*. 1996;316:171–179.
32. Phillis JW, Smith-Barbour M, O'Regan MH, et al. Amino acid and purine release in rat brain following temporary middle cerebral artery occlusion. *Neurochem Res*. 1994;19:1125–1130.
33. Andine P. Involvement of adenosine in ischemic and postischemic calcium regulation. *Mol Chem Neuropathol*. 1993;18:35–49.
34. Xu XH, Zhang SM, Yan WM, et al. Development of cerebral infarction, apoptotic cell death and expression of X-chromosome-linked inhibitor of apoptosis protein following focal cerebral ischemia in rats. *Life Sci*. 2006;78: 704–712.
35. D'Alimonte I, Ballerini P, Nargi E, et al. Staurosporine-induced apoptosis in astrocytes is prevented by A1 adenosine receptor activation. *Neurosci Lett*. 2007;418:66–71.
36. Ngai AC, Coyne EF, Meno JR, et al. Receptor subtypes mediating adenosine-induced dilation of cerebral arterioles. *Am J Physiol Heart Circ Physiol*. 2001; 280:H2329–H2335.
37. Zhou AM, Li WB, Li QJ, et al. A short cerebral ischemic preconditioning upregulates adenosine receptors in the hippocampal CA1 region of rats. *Neurosci Res*. 2004;48:397–404.

Clinical Neurophysiology 123 (2012) 1496–1501

Contents lists available at SciVerse ScienceDirect

Clinical Neurophysiology

journal homepage: www.elsevier.com/locate/clinph

sLORETA-qm for interictal MEG epileptic spike analysis: Comparison of location and quantity with equivalent dipole estimation

T. Uda [a,*], N. Tsuyuguchi [a], E. Okumura [b], S. Sakamoto [c], M. Morino [d], T. Nagata [a], H. Ikeda [a], N. Kunihiro [a], T. Takami [a], K. Ohata [a]

[a] Department of Neurosurgery, Osaka City University Graduate School of Medicine, Osaka, Japan
[b] MEG Gr. Bio and Analytical Center, Yokogawa Electric Corporation, Kanazawa, Japan
[c] Department of Radiology, Osaka City University Graduate School of Medicine, Osaka, Japan
[d] Department of Neurosurgery, Tokyo Metropolitan Neurological Hospital, Tokyo, Japan

ARTICLE INFO

Article history:
Accepted 14 December 2011
Available online 31 January 2012

Keywords:
sLORETA
Equivalent current dipole
Epilepsy
Interictal spike
MEG

HIGHLIGHTS

- Magnetic source location and quantity were compared between quantitative modification of a standardised low-resolution brain electromagnetic tomography (sLORETA-qm) and equivalent current dipole (ECD) for analysis of the interictal epileptic spike.
- sLORETA-qm closely correlated with ECD concerning point source location and quantity.
- sLORETA-qm is a reliable quantifiable method without arbitrariness that can be used for analysis of the interictal epileptic spike.

ABSTRACT

Objective: To determine whether quantitative modification of a standardised low-resolution brain electromagnetic tomography (sLORETA-qm) could be used as a reliable tool for quantitative analysis of magnetoencephalography (MEG) for analysis of the interictal epileptic spike. To verify the performance of sLORETA-qm, magnetic source location and quantity were compared with the equivalent current dipole (ECD) method.

Methods: A total of 50 sources from 10 patients with epilepsy were obtained. Analyses were performed after the MEG data were 3–70 Hz band-pass filtered. Time points for analysis were selected referring to waveform patterns and the isofield contour map. With the same spherical model, source estimation was conducted with two methods of analysis: ECD and sLORETA-qm. Distance from the centre of the spherical model and intensities were compared between the methods.

Results: There were no significant differences between the methods in the distance from the spherical model (paired t-test, $p = 0.8761$). Source intensities between the methods were strongly correlated (Spearman's Rho = 0.9803, $p < 0.001$).

Conclusions: sLORETA-qm was closely correlated with ECD concerning point source location and quantity in analysis of the interictal epileptic spike.

Significance: sLORETA-qm is a reliable quantifiable method without arbitrariness for analysis of the interictal epileptic spike.

1. Introduction

An epileptogenic zone is defined as the zone of actual seizure onset that needs to be removed in order to achieve seizure freedom (Penfield and Jasper, 1954). In preoperative evaluation of epilepsy, it is preferable to record the ictal epileptiform discharge in electroencephalography (EEG) or magnetoencephalography (MEG) in order to detect the epileptogenic zone. Chances to record a seizure from a patient are rather low because of limited recording time; so it is important to detect the irritative zone that demonstrates the interictal focal epileptiform discharge due to paroxysmal neuronal activity.

Paroxysmal interictal epileptiform discharge generates a strong magnetic flux compared to normal spontaneous magnetic activity of the brain. For analysis of interictal epileptiform discharge, the equivalent current dipole (ECD) estimation method is commonly

* Corresponding author. Address: Department of Neurosurgery, Osaka City University Graduate School of Medicine, 1-4-3 Asahi-machi, Abeno-ku, Osaka 545-8585, Japan. Tel.: +81 6 6645 3846; fax: +81 6 6647 8065.
E-mail address: uda@med.osaka-cu.ac.jp (T. Uda).

1388-2457/$36.00 © 2011 International Federation of Clinical Neurophysiology. Published by Elsevier Ireland Ltd. All rights reserved.
doi:10.1016/j.clinph.2011.12.008

used, especially for clinical evaluation. In this method, a single source at a single time point is estimated from the surface magnetic field distribution, and the location, intensity and orientation of the source are obtained.

Although the ECD estimation method is a simple and useful model for solving the electromagnetic inverse problem, it has two problems concerning objective assessment of the electromagnetic activity: restricted numbers of current sources and arbitrary sensor selection.

Spatial filtering techniques are alternative approaches to these problems. Standardised low-resolution brain electro-magnetic tomography (sLORETA) is a non-adaptive spatial filtering technique that has been reported previously (Pascual-Marqui, 2002), and has no localisation bias under ideal conditions (Greenblatt et al., 2005; Sekihara et al., 2005). This technique can be used to determine the localisation of magnetic activities, even for multiple sources (Wagner et al., 2004), unless the sources are located in close proximity to each other. Furthermore, source reconstruction by sLORETA can be performed without sensor selection, and therefore arbitrariness of sensor selection can be avoided. Moreover, sLORETA can also provide pseudo-statistic values, which can be used as estimates of the degree of activity. These properties are highly advantageous for quantitative analysis of MEG in a clinical setting.

To establish sLORETA as a quantifiable method, sLORETA was modified and named sLORETA-qm (Terakawa et al., 2008). The use of sLORETA-qm with the somatosensory evoked field (SEF) has been reported previously (Terakawa et al., 2008). According to that report, the ECD moment and sLORETA-qm intensity were highly correlated with the SEF. Moreover, sLORETA-qm was applied to assess spontaneous neuromagnetic slow wave activity (Sakamoto et al., 2010). In that report, neuromagnetic slow wave activity was demonstrated to be distributed in the area of ischaemic brain lesions, and the activity intensity decreased after surgery performed to improve cerebral blood flow. It has been reported that sLORETA-qm may offer a novel, non-invasive method for identification and quantification of cerebral ischaemia. However, it remains unclear whether this modification of sLORETA can be applied to the interictal epileptic spike discharge, in other words, spontaneous paroxysmal magnetic activity without averaging.

The present study was performed to determine whether sLORETA-qm spatial filtering could be used as a reliable tool for quantitative analysis of the MEG interictal epileptic spike discharge. To verify the performance of sLORETA-qm, magnetic source location and quantity were compared with the conventional ECD method.

2. Methods

2.1. Patients

All 10 patients (six men and four women, ranging in age from 20 to 55 years) with medically refractory partial epilepsy and demonstrating interictal epileptic spike discharges in EEG and MEG, who were admitted to Department of Neurosurgery, Osaka City University Hospital between May 2008 and March 2010 and met the following inclusion criteria, were retrospectively included in the study. Patient characteristics are shown in Table 1. They all had epilepsy surgery at Osaka City University Hospital after MEG, and were followed up for at least 1 year after surgery. All subjects gave their informed consent, and the study was approved by the Ethics Committee of Osaka City University Hospital.

2.2. MEG measurement protocol

MEG was performed in a magnetically shielded room at Osaka City University Hospital using a 160-sensor helmet-type MEG system (Yokogawa Electric Corporation, Tokyo, Japan) with a magnetic field resolution of 4 fT/Hz1/2 in the white noise region. Sensing and reference coils in this system are both 15.5 mm in diameter, with a 50-mm baseline and 23 mm of separation between each pair of sensing coils. The subjects were positioned in the supine position with their eyes closed, with use of a horizontal-type dewar. MEG data were recorded through a 1- to 200-Hz band-pass filter with a sampling rate of 1000 Hz. The MEG acquisition time was 20 min. In addition, 19 electroencephalography (EEG) leads were recorded simultaneously, according to the international 10–20 system.

Table 1
Patient characteristics and spike origin.

Case	Age (years)	Gender	Spike origin
1	23	M	bil T
2	32	M	Lt T
3	55	M	Lt F
4	38	M	Rt F
5	28	F	Lt F
6	24	F	Rt T, Rt F
7	20	F	Rt F, Rt T, Lt O
8	30	M	bil T
9	47	F	bil O, Rt T
10	34	M	Rt T

M, male; F, female; bil, bilateral; Rt, right; Lt, left;T, temporal; F, frontal; O, occipital.

2.3. Data analysis

To reduce noise caused by the surrounding environment, data from the reference magnetometers, which were located outside of the dewar and picked up only environmental noise, were subtracted from the obtained MEG data.

As an epileptic spike discharge is defined as having a duration of 20 to less than 70 ms (IFSECN, 1974), the MEG data were band-pass filtered to cover this duration between 3 and 70 Hz (Papanicolaou, 2009). Time points for analysis were selected referring to the waveform patterns of MEG and EEG, and the isofield contour map of MEG. The following two methods of analysis, ECD and sLORETA-qm, were conducted using the same spherical model. Three-dimensional coordinates, distance from the centre of the spherical model and intensities were obtained by the two analytical methods and recorded for analysis.

2.3.1. ECD

Twenty sensors around the centre of the maximum extremum (the point at which the magnetic flux exits) and the minimum extremum (where the flux re-enters the head) on the isofield contour map were selected, and a magnetic source was estimated at a selected time point with the single dipole estimation method (Cuffin, 1985; Scherg and Von Cramon, 1986). Dipoles estimated with over 90% goodness of fit (GOF) were adopted as successful source estimations.

2.3.2. sLORETA-qm

MEG data from all sensors (160 sensors) were used for analysis. The brain area in the spherical model was divided into approximately 13,000 voxels with a spacing of $5 \times 5 \times 5$ mm^3. The actual voxel count depended on the head size of each subject, and ranged from 11,668 to 18,796. Voxels in areas with no effect of brain activities in the cerebral cortex (such as the cerebellum, brain stem, and in the vicinity of the eyes) were excluded. Voxels within 25% of the radius of the spherical model were also excluded. These operations were performed automatically by referring to the spherical model of each subject. In Fig. 1, adopted voxels are shown in pink. Previous reports have described how to obtain quantitative multiple

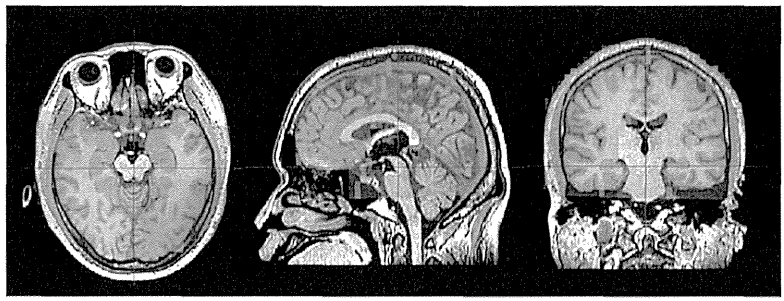

Fig. 1. Brain area in the spherical model is divided into voxels with a volume of $5 \times 5 \times 5$ mm^3. Adopted voxels are shown in pink. Voxels in areas with no effect from brain activities in the cerebral cortex (such as cerebellum, brain stem, and the vicinity of the eyes) are excluded. Voxels within 25% of the radius of the spherical model are also excluded.

source estimation using sLORETA-qm (Sakamoto et al., 2010; Terakawa et al., 2008). In short, the source reconstruction was performed by sLORETA at each time point as a first step (Pascual-Marqui, 2002). Subsequently, a voxel with a spatially maximum or local maximum intensity at each time point was chosen as a peak source. Finally, on the voxel chosen as the peak source, the quantified source intensity was estimated by correcting the lead-field component. The centre of the voxel was used as the three-dimensional coordinate. Source estimation with sLORETA-qm was computed with custom software developed using MATLAB version 7.7 (MathWorks Inc., Natick, MA, USA).

2.4. Evaluation

If the distances between the sources in the two analytical methods [(a) in Fig. 2] were less than 5 mm (same as the voxel diameter), these sources were considered concordant. In order to compare the location of the source between the two methods of analysis, distances from the centre of the spherical model [(b) and (c) in Fig. 2] were measured for each spike. A paired sample t-test was used to identify differences in distance from the spherical centre between the two methods after confirming the data were normally distributed (assessed by the Shapiro–Wilk test).

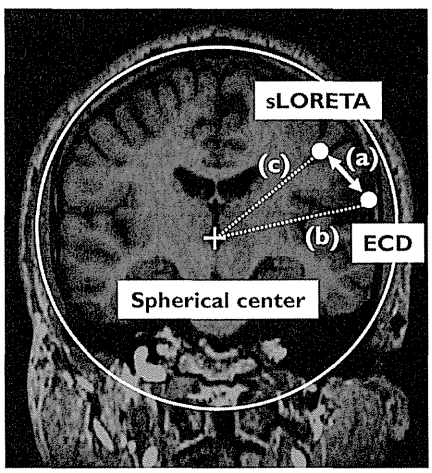

Fig. 2. Summary of analysed parameters: (a) distances between sources estimated by the equivalent current dipole (ECD) and by quantitative modification of standardised low-resolution brain electromagnetic tomography (sLORETA-qm), (b) distance from the centre of the spherical model to the source estimated by ECD, and (c) distance from the centre of the spherical model to the source estimated by sLORETA-qm. Circle indicates the radius of the spherical model.

To study the relationships of the intensities between the two methods, a non-parametric correlation coefficient (Spearman's Rho) was used because the intensities of the two methods were not normally distributed (Shapiro–Wilk test). Probability values less than 0.05 were considered significant in all statistical analyses. The software JMP 9.0 for Windows (SAS Institute Inc., Cary, NC, USA) was used for statistical evaluation.

3. Results

A total of 50 concordant sources (five interictal epileptic spikes for each patient) were used for analysis. The distance between the corresponding two sources [(a) in Fig. 2] and source intensities from the two methods are summarised in Table 2.

3.1. Distance from the centre of the spherical model to the estimated sources

The distances from the centre of the spherical model to the estimated sources were 57.95 ± 12.96 mm (mean ± SD) in ECD and 57.99 ± 12.81 mm (mean ± SD) in sLORETA-qm [(b) and (c) in Fig. 2, respectively]. There were no significant differences between the two distances (paired sample t-test, $p = 0.8761$).

3.2. Source intensities

As a result of correlation analysis, a close correlation was found between the two source intensities (Spearman's correlation coefficient, Rho = 0.9619, $p < 0.001$) (Fig. 3).

3.3. Representative case

3.3.1. Case 1_23-year-old man

The overlaid waveform of all 160 sensors is shown in Fig. 4A. High-amplitude magnetic flux was recorded around the time point of 1597 ms. In Fig. 4B, the isofield contour map at the time point of 1597 ms was depicted. The maximum extremum and the minimum extremum were recognised in the left temporal area. In ECD, 20 sensors around the centre of the maximum extremum and minimum extremum were selected (blue dots and sensor numbers in Fig. 4B). Waveforms of the 20 selected sensors are shown in Fig. 4C. Magnetic sources were estimated with the single dipole estimation method. The source was estimated with 94.56% GOF and the intensity of the source was 137.77 nAm. The distance from the spherical centre was 55.53 mm. In sLORETA-qm, all 160 sensors were used for source estimation. A total of three sources could be estimated, and the source intensities were 164.05, 66.19, and 39.80 nAm (Fig. 5). The peak voxel was located in left temporal lobe [(a) in Fig. 5] and the distance from the spherical